communications engineering

Article

https://doi.org/10.1038/s44172-024-00333-x

Human-structure and human-structure-human interaction in electro-quasistatic regime

Samyadip Sarkar[1,3], David Yang[1,3], Mayukh Nath[1], Arunashish Datta[1], Shovan Maity[2] & Shreyas Sen[1]

Augmented living equipped with electronic devices requires widespread connectivity and a low-loss communication medium for humans to interact with ambient technologies. However, traditional radiative radio frequency-based communications require wireless pairing to ensure specificity during information exchange, and with their broadcasting nature, these incur energy absorption from the surroundings. Recent advancements in electroquasistatic body-coupled communication have shown great promise by utilizing conductive objects like the human body as a communication medium. Here we propose a fundamental set of modalities of non-radiative interaction by guiding electroquasistatic signals through conductive structures between humans and surrounding electronic devices. Our approach offers pairing-free communication specificity and lower path loss during touch. Here, we propose two modalities: Human-Structure Interaction and Human-Structure Human Interaction with wearable devices. We validate our theoretical understanding with numerical electromagnetic simulations and experiments to show the feasibility of the proposed approach. A demonstration of the real-time transfer of an audio signal employing an human body communications-based Human-Structure Interaction link is presented to highlight the practical impact of this work. The proposed techniques can potentially influence Human-Machine Interaction research, including the development of assistive technology for augmented living and personalized healthcare.

Rapid advancements in information-communication technologies (ICT) have expedited the growth of Human-Machine Interaction (HMI) research over the last few decades. The societal impact of growth in the versatile HMI field is not limited to but encompasses the following: connected healthcare in 'smart' hospitals, ease of information exchange between the attendees during a meeting or in any other social gatherings[1,2], widespread connectivity in smart-home assisted independent living[3–6], secure biometric authentications[7–12] etc. The demand for an interface with specificity in communication through which humans can interact with ambient intelligence with convenience is one of the primary aspects that drive HMI research[13]. These prompt the exploration of such an interface that facilitates augmented living using electronic devices powered by the Internet of Things (IoT)[14–16]. Besides, devices in the form of wearables, implantable, ingestible, etc., that form a network of IoT-enabled interconnected devices while sharing the human body as a communication medium, namely Internet of Bodies (IoB)[17,18], attempt to raise living standards while ensuring user safety. Previously proposed various studies on the interaction of IoB devices with IoT-enabled assisting technologies use radiative wireless communication such as Bluetooth, Med-Radio, WiFi, etc., which requires wireless pairing while ensuring specificity, suffer from security vulnerabilities (i.e., signal availability extends about 5–10 m distance around the human body). Besides security constraints, the limited battery capacity[19] of small form factor wearable IoB devices prompts the requirement of ultra-low power (sub μW to μW power levels) circuits. With its improved energy efficiency (~sub-10 pJ/bit) and enhanced physical security (i.e., signal leakage constrained within 1 cm from the body surface and within 15 cm from an EQS-HBC device)[20,21], Electro-Quasistatic Human Body Communication (EQS-HBC)[2,20,22,23], depicted in Fig. 1a, has emerged as a promising alternative to the RF-based wireless communication for the IoB-enabled devices.

Touch is a natural medium for humans to interact with their surrounding electronic devices, and hence exploring sensing-communication modalities involving touch-based phenomena and augmenting those with emerging technologies to enhance its applicability towards user convenience has intrigued researchers over the last couple of decades[24–26]. Previous

[1]School of Electrical and Computer Engineering, Purdue University, West Lafayette, IN, USA. [2]Quasistatics Inc., West Lafayette, IN, USA. [3]These authors contributed equally: Samyadip Sarkar, David Yang. e-mail: shreyas@purdue.edu

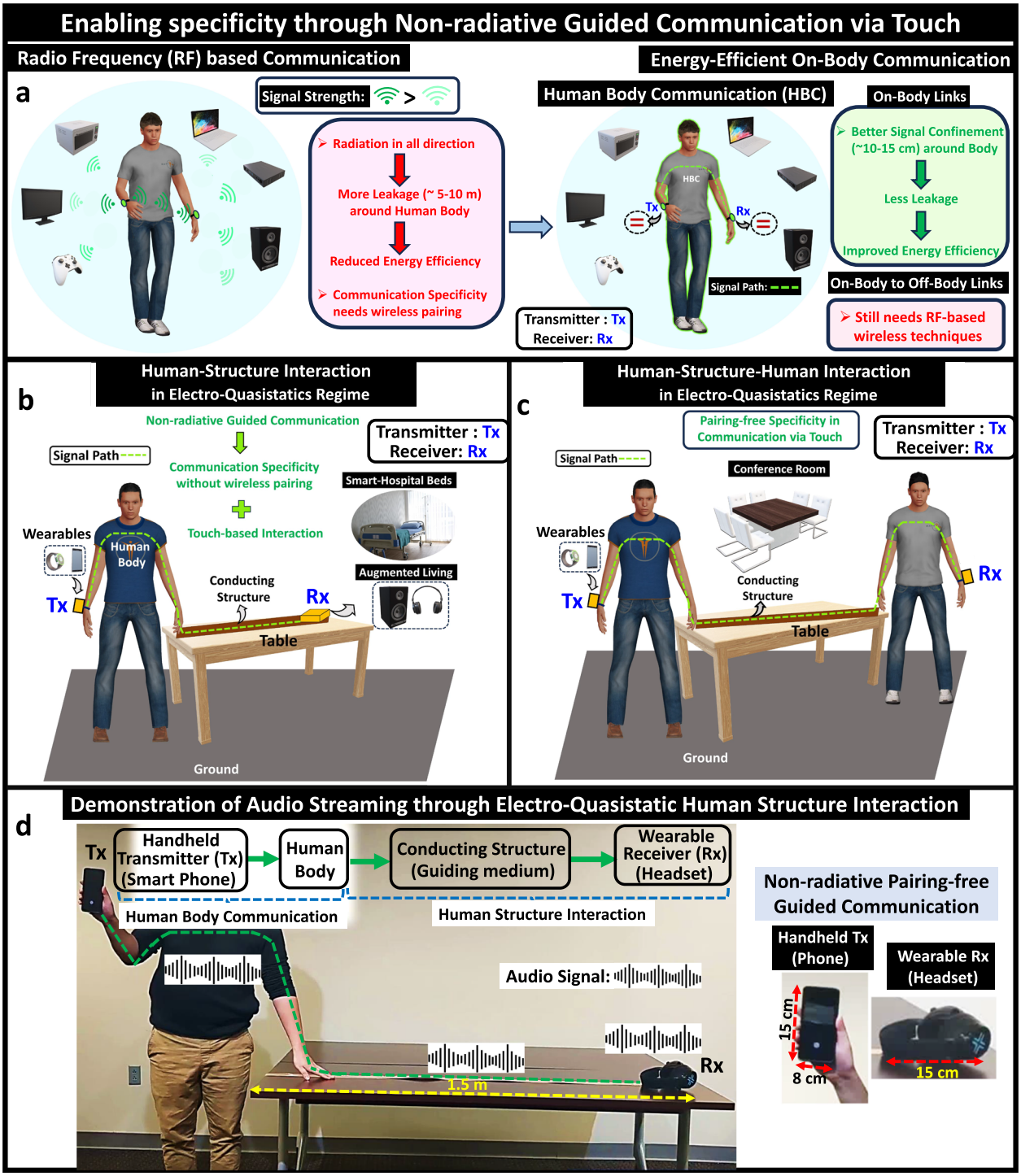

Fig. 1 | Need for energy-efficient non-radiative guided communication with specificity. a Radio frequency (RF)-based radiative communication: higher leakage and needs wireless pairing. Non-radiative guided interaction in electro-quasistatics (EQS): **b** Human-Structure Interaction (HSI). **c** Human-Structure-Human Interaction (HSHI). Guided communication via conducting structure (CS) offers specificity during touch. **d** Demonstration of audio streaming via EQS Human Structure Interaction (HSI) link. Human figures are made in the Open-source software MakeHuman.

studies in the field of Human-Computer Interaction (HCI) that utilize touch-based communication can be broadly classified under the following four categories[13]: Electric Field Sensing, Gesture Recognition, Biometrics, and Human Body Communication (HBC).

The following subsection summarizes the cardinal attributes of the prior arts on the touch-based body-coupled communication that can be broadly classified under the following categories: (a) System & Circuit-level implementation, and (b) Channel Characterization of HBC.

Studies on system & circuit-level implementation. A system that allows users to dynamically personalize the nearby environment (i.e., personalizing a ubiquitous computer) via exchanging a wearable digital key through the user's body simply during touch was presented[12]. However, with its principle of operation being near-field technology called TouchNet, this interaction modality cannot support long-range on-body-to-off-body communication links for humans to interact with ambient intelligence. Utilizing the floor surface and the human body as an Ethernet cable, a

wireless-like broadband networking and positioning system for indoor places, namely CarpetLAN, working on the principle of weak electric field interaction was introduced[27]. Nevertheless, the large size (1000 cm^3) of the demonstrated prototype node unit makes this technique power-hungry (8 W). Using intrabody communication, an intuitive context-aware service, namely Touch-And-Play (TAP), for the interaction between multimedia devices was demonstrated[28]. The touch-based communication link with limited coverage still has to rely on wireless techniques (like WiFi) to enable user interaction with devices located at far distances. An interactive ball game (Earthlings Attack) that utilizes the principle of HBC when an active ball device with a built-in transmitter comes in contact with the user body and sends information to the wearable receiver belt was described[29]. Relying on the capacitively coupled body communication, commodity devices like fingerprint sensors and touchpads, while residing around the human body, can wirelessly transmit information to battery-powered wearable receivers, was shown[30]. With modulation schemes of the input devices, this method supports a data rate of up to 50 bps over the human body, which can support authentication applications but is not adequate for transferring information. Introducing a sensing approach for the skin to act as a continuous touch-tracking surface, a wearable system (SkinTrack), that consists of a ring as a transmitter that emits an AC signal at a frequency of 80 MHz into the finger on which it is worn, and a wristband with patterned electrodes at the opposite arm, acting as the receiver, was proposed[25]. During touch-based interactions, measurement of the phase differences across different electrode pairs enables real-time touch tracking. However, this study does not cover the analysis of physical phenomena from the variability in propagation characteristic of the 80 MHz electromagnetic (EM) waves around the human body. Presenting various scenarios of the subject interaction with infrastructures based on body channel communication (BCC), the design and a prototype implementation of the TouchCom-based platform: a simple transceiver that relies on software-centered processing, was presented[31]. The offered data rate, though adequate for gaming, localization, and identification purposes, is not enough to support high-quality audio and video streaming. Utilizing Bodywire-HCI, non-radiative strictly touch-based communication in EQS regime can be achieved through signal confinement and highlighted the benefits of touch-based communication using EQS signaling was proposed[13]. However, enabling the communication between humans and electronic objects that are at distant locations in an EQS regime (i.e., enabling on-body-to-off-body links with large communication coverage) was beyond the scope of this work. Besides the system-level demonstration of HBC, there have been studies focused on the energy-efficient custom integrated circuit design for HBC-enabled applications[32–35]. The comparison of the above-mentioned works with the proposed modality is summarized in Table 1:

Studies on body channel characterization. In addition to the rapid advancements in the system and circuit-level implementation of HMI-enabled applications, the domain of channel characterization of capacitive coupling-based HBC has also experienced exponential growth. Developing an understanding of the channel variability from the following: the ground connection, parasitic return paths between the device's floating ground to earth ground[36–38], excitation and termination modalities and impedances[36,39,40], and the influence of external objects[41], using battery-powered wearable devices have proven to be useful as it has unveiled immense possibilities of enabling interaction modalities between humans and the ambient technologies.

Hence, given the need for a non-radiative communication link between humans and surrounding electronic devices, we propose a fundamentally new set of interaction modalities while preserving the signal confinement benefits of EQS-HBC around the human body, enabling guided communication by driving EQS signals through conductive structures (CS) during touch-based HMI, illustrated in Fig. 1c. Besides, selectivity in communication can be achieved naturally during touch by patterning the CS accordingly. These can potentially facilitate pairing-free simultaneous data transfer to multiple intended recipients in meetings or any other social gatherings, which is otherwise not possible with Bluetooth, which requires wireless pairing that adds complexity to the pairing interface with an increased no. of devices. Among the different coupling modalities of HBC[42–45], this paper relies on the principle of EQS capacitive coupling for its frequency-independent nearly consistent path loss across the entire channel (with high impedance capacitive termination at the receiver), making it suitable for long-distance communication like in an on-body-to-off-body link with coverage ranges in ~3–5 m. On the contrary, the galvanic mode of communication, besides not being an optimum choice from the user's safety viewpoint[23] because of driving higher current between the transmitter electrodes, cannot support long channels owing to its principle of operation is the dipole-dipole interaction that causes its channel gain to keep on decreasing away from the transmitter and vary with dipole separation and their relative orientation[41]. Furthermore, the human body, being transparent to the quasistatic magnetic field (frequency <~30 MHz) and the channel gain to keep on sharply falling with the relative separation and the alignment mismatch between the transmitter and receiver coils, makes the magnetic HBC not suitable for long-range communication with wearable devices[45].

A limited number of studies on modeling the communication channel for capacitive Human-Structure coupling demand a comprehensive analysis using wearable devices. In the EQS regime (≤10 MHz), where the operating wavelength ($\lambda \geq 30$ m) of signals in air is much larger than the dimensions of the communicating devices (≤0.04 m), the human body (≤2 m) and the incorporated CS (~1 m), it is consistent to approximate the existing distributed coupling capacitances with their lumped counterparts. From the understanding of the previously proposed lumped elements-based bio-physical models[37–39] for capacitive HBC in EQS, this paper develops generalized equivalent circuit models for capacitive Human-Structure Interaction (HSI) and Human-Structure-Human Interaction (HSHI). In capacitive HSI and HSHI, while the human body and the conducting structure constitute the forward path for signal transmission, the parasitic capacitances resulting from the capacitive coupling between the HBC device's floating ground and the earth's ground form the return path of the channel. Besides, presenting a systematic analysis of the interaction modalities, a real-time streaming of audio signal utilizing HBC-HSI link is demonstrated in this paper, as shown in Fig. 1d.

The **Technical advancement through EQS HSI& HSHI** is summarized below:

Extended Communication Coverage. The work extends the principle of EQS capacitive HBC-based on-body links (communication coverage limited to the human body dimension ≤2m) to the on-body-to-off-body links (more coverage) with wearable devices to enable interactions between humans and ambient technologies by introducing a conducting structure as a medium for guided communication. Communication links with higher coverage can potentially inspire the emergence of energy-efficient HSI applications to facilitate augmented living.

Characterization of an on-body-to-off-body channel for reliable communication. The received signal strength, in other words, the introduced loss in the communication channel from the user's body and the guiding medium depends on different factors. The channel characterization is performed for varying receiver positions on the conducting structure (CS) relative to the human body through FEM-based numerical simulations and experiments. Besides, the benefits of touch-based interactions over capacitively coupled interactions under non-touching scenarios are illustrated. Furthermore, the effect of dimensional variation and patterning of the CS as a guiding medium on the channel characteristics are analyzed comprehensively to optimize the channel behavior. These understandings are invaluable in determining the link coverage, the sensitivity of the receiver, and the adequate data rate for reliable communication.

Developing Circuit Model-based understanding. Analyzing the variability of a communication channel also requires understanding the physics behind the proposed interaction modality that facilitates identifying the decisive channel parameters toward optimizing the link. Hence, simplified lumped elements-based circuit models are developed to capture the root causes of channel variability in EQS HSI and HSHI and are analyzed in detail.

Table 1 | Comparison of Electro-Quasistatic Human Structure Interaction (EQS HSI) with the prior techniques for touch-based body-centric applications: EQS HSI is the first system that enables energy-efficient touch-based guided interaction for an on-body-to-off-body link with larger communication coverage

Author : Technology	Operating frequency (MHz) & bitrate (bps)	Operating principle	Channel modeling & theoretical understanding	Link type & coverage range	Demonstrated applications
Matsushita et al.: Wearable Key	10 & 14 MHz, 9.6 kbps	Exchange of wearable key during personalization through touch	No	On-to-off body limited coverage (near field)	Personalization of ubiquitous computer
Fukumoto et al.: CarpetLAN	10 Mbps	Electric field based transmission	No	Range ~1 m (increasing coverage increases power consumption)	Indoor positioning & detection of human and smart appliances
Park et al.: TAP: Touch-And-Play	1 Mbps	Touch to establish connection between multimedia devices	No	Limited coverage (Touch-based)	User with a digital camera touches HDTV to display & touches printer to print photo file
Takahashi et al.: Earthlings Attack	100's kHz–MHz, 500–700 kbps	Information transfer via injecting microcurrent through body	No	Off-to-on body	Ball game interaction using HBC
Hessar et al.: On-Body Transmissions with Commodity Devices	25–50 bps	Capacitive-coupling-based communication	Yes	On-to-off body (near) limited coverage	Fingerprint sensors & touchpads transmitting information to an on-body wireless receiver
Zhang et al.: SkinTrack	80 MHz	EM waves propagating along a physical waveguide, i.e., human arm	No	Limited range	Real-time touch tracking
Varga et al.: Interactive Infrastructure via Body Channel Communication (BCC)	8 MHz, 21.875 kb/s	Data transfer via coupled E-Field	No	On-to-off body	ConquerIt, MusicBand, TrackMe, LightUp
Maity et al.: BodyWire-HCI	500 kHz–20 MHz, 8 kbps	EQS HBC-HCI (strictly touch)	No	On-to-off body guided (Near), Range limited by the contact area of the Rx electrode	Image transfer, unlocking computers via body-worn keys during touch-based events
This work: EQS HSI & HSHI	(a) 1 MHz (For Simulation) & 1.53 MHz (For Experiments), (b) 18.75 MHz, 1.44 Mbps (For audio demo)	EQS HBC-HSI: guided communication (touch-based)	Yes	On-to-off body guided (Near & Far). i.e., Larger Coverage: ~3 m (HSI), ~5 m (HSHI)	Audio streaming via On-to-Off Body link

Evaluation of signal leakage in an on-body-to-off-body communication link. The specificity in information exchange through a communication channel demands non-radiative guided interaction with minimum leakage. This article covers the leakage measurements around the CS and its variability with various ways of user interaction that offer an estimate of the signal-to-noise ratio (SNR) for the different receiver positions relative to the user's body to ensure selectivity during communication.

Advancement in demonstrated applications. This work introduces real-time data transfer (~Mbps) and specificity by utilizing the EQS HBC-HSI link via the demonstration of audio streaming through the human body and a CS with battery-powered wearable communicating devices. Relying on the principle of EQS capacitive body-coupled communication, the audio streaming happens seamlessly as the user with a wearable transmitter (smartphone) stands very close or touches the CS on which the wearable headset as the receiver is placed.

For **Electro-quasistatic (EQS) capacitive inter-object coupling**, the signal transmission at lower frequencies (10's of MHz or even less) can be quasi-statically approximated to be electrical in nature. Now, to utilize the signal confinement benefits of non-radiative communication in EQS regime[20], the proposed modalities: Human-Structure and Human-Structure-Human Interaction are considered to use EQS signaling.

In **EQS human-structure interaction (HSI)**, the voltage couplers (i.e., signal electrodes) at the transmitting and receiving ends are connected to the human body and the CS respectively, whereas the respective ground electrodes are left floating. Based on the positioning of the receiver on CS relative to the human body and whether the human touches the CS, this interaction modality can be analyzed as follows: In the absence of the CS, the human body, with its conductive tissue properties forms the forward path, and existing parasitic capacitances between the devices (Tx and Rx) ground-to-earth's ground form the return path, shown in Fig. 2a. Owing to the strict confinement of the EQS signal, the weak capacitive coupling, decided by the Rx position relative to the human body, determines the output voltage. However, this non-guided mode suffers from high end-to-end channel loss. To alleviate this issue, the incorporation of a structure with high enough electrical conductivity (i.e., σ comparable to metals) between the communicating objects ensures a guided nature of the coupled EQS field by making the forward path of signal transmission through the body and structure (CS), which can be schematically pictured, shown in Fig. 2b.

The CS as a guiding medium, offers wireline-like benefits in terms of energy efficiency and signal confinement during touch, shown in Fig. 2c. Based on the understanding of the involved capacitive couplings in HBC from the previously proposed bio-physical models[37–39], we present a simplified equivalent circuit model for HSI in EQS, shown in Fig. 2d. For on-body-to-off-body link coverage (i.e., $l = l_{Body} + l_{CS}$, where l_{Body} (≤2m) represents length of the on-body link and l_{CS} designates the length of the CS or off-body-link) to be the order of magnitude lower than the operating wavelength in the air (λ_0) i.e., $l << \lambda_0$ in EQS frequency regime, with high enough σ, the guiding structure is effectively regarded as a single node in the equivalent circuit model that contributes to the coupling capacitance from the structure to the ground (C_{SG}). Besides the parasitic return path capacitances ($C_{xTx} = xC_{GTx}$ and $C_{yRx} = yC_{GRx}$) at the Tx and Rx end, which depend upon the device size (i.e., C_{GTx}, $C_{GRx} = 8\epsilon_0 a$, where a = radius of disk-shaped devices) and their positioning (i.e., x and y relative to the body and CS respectively), the following capacitances: Body-to-CS (C_{SB}) and CS-to-Earth's ground (C_{SG}), decided by their relative separation (d) and the dimension of the CS play a crucial role in deciding the channel characteristic. Hence, with voltage mode capacitive division, the approximated transfer function for the simplified equivalent circuit model can be represented as follows:

$$\frac{V_{out}}{V_{in}} \approx \frac{C_{xTx}}{C_B} \times \frac{C_{SB}}{C_{SB} + C_{SG}} \times \frac{C_{yRx}}{C_{L(eff.)}} \quad (1)$$

where,

$$C_{L(eff.)} = C_{GBRx} + C_{GSRx} + C_L \quad (2)$$

which shows that by maximizing the return path capacitances at the Tx and Rx, i.e., C_{xTx}, C_{yRx} together with structure-to-body coupling, i.e., C_{SB} through touch while minimizing C_{SG} and $C_{L(eff.)}$, an optimized channel gain can be achieved. Comparative analysis of the depicted scenarios in Fig. 2, illustrates that the presence of a CS between communicating devices can improve the received signal level, which can be eventually maximized through touch.

In **EQS human-structure-human interaction (HSHI)**, the signal electrodes of the Tx and Rx devices are on the human body with their respective ground electrodes left floating. Different types of capacitive couplings in EQS-HSHI, are presented in Fig. 3. In the absence of the CS, the two bodies, weakly coupled by the inter-body coupling, shown in Fig. 3a, form the forward path of signal transmission[21]. This non-guided mode suffers from high loss and security limitations since non-intended recipients present nearby can easily snoop on the data. Aiming to strengthen the inter-human communication link, a CS as a guiding communication channel, is introduced in between. Incorporation of a CS between two humans while neither of them touches the structure, boosts the received signal level with the combination of inter-body coupling (C_C) and body-to-structure couplings (C_{SBTx} and C_{SBRx}) on either end. Two human bodies, together with the CS, form the forward path, and parasitic capacitances, present between the Tx and Rx ground planes and the earth's ground form the return path, depicted in Fig. 3b. Similar to the HSI, wireline-like benefits in received signal level, are obtained when both humans touch the CS, depicted in Fig. 3c. A generalized simplified equivalent circuit model for HSHI in EQS is illustrated in Fig. 3d. The transfer function of the proposed simplified equivalent circuit can be approximately formulated in Eq. (3) as follows:

$$\frac{V_{out}}{V_{in}} \approx \frac{C_{xTx}}{C_{B1} + C_1} \times \frac{C_E}{C_E + C_2 + C_{B2}} \times \frac{C_{xRx}}{C_{L(eff.)}} \quad (3)$$

where,

$$C_1 = \frac{C_{SBRx} C_{SG}}{C_{SBRx} + C_{SG} + C_{SBTx}} \quad (4)$$

$$C_2 = \frac{C_{SBTx} C_{SG}}{C_{SBRx} + C_{SG} + C_{SBTx}} \quad (5)$$

$$C_3 = \frac{C_{SBTx} C_{SBRx}}{C_{SBRx} + C_{SG} + C_{SBTx}} \quad (6)$$

$$C_E = C_C + C_3 \quad (7)$$

$$C_{L(eff.)} = C_{GBRx} + C_L \quad (8)$$

With the above-mentioned theoretical postulation, the following sections have attempted to substantiate the understandings initially by FEM-based simulations and eventually through real-time measurements.

Results

Based on the discussed interaction modalities, this section illustrates the FEM-based simulation and measurement results of capacitive-coupling-based HSI and HSHI in EQS regime.

FEM simulation results

To confirm the theoretical understanding of the communication channel characteristics, here we present the results from EM simulations executed in ANSYS high frequency structure simulator (HFSS). A simplified human body model is employed, whose accuracy has been confirmed through comparison with a more detailed model in a previous study[23]. With an applied input excitation as an ideal AC voltage source of amplitude 1 V,

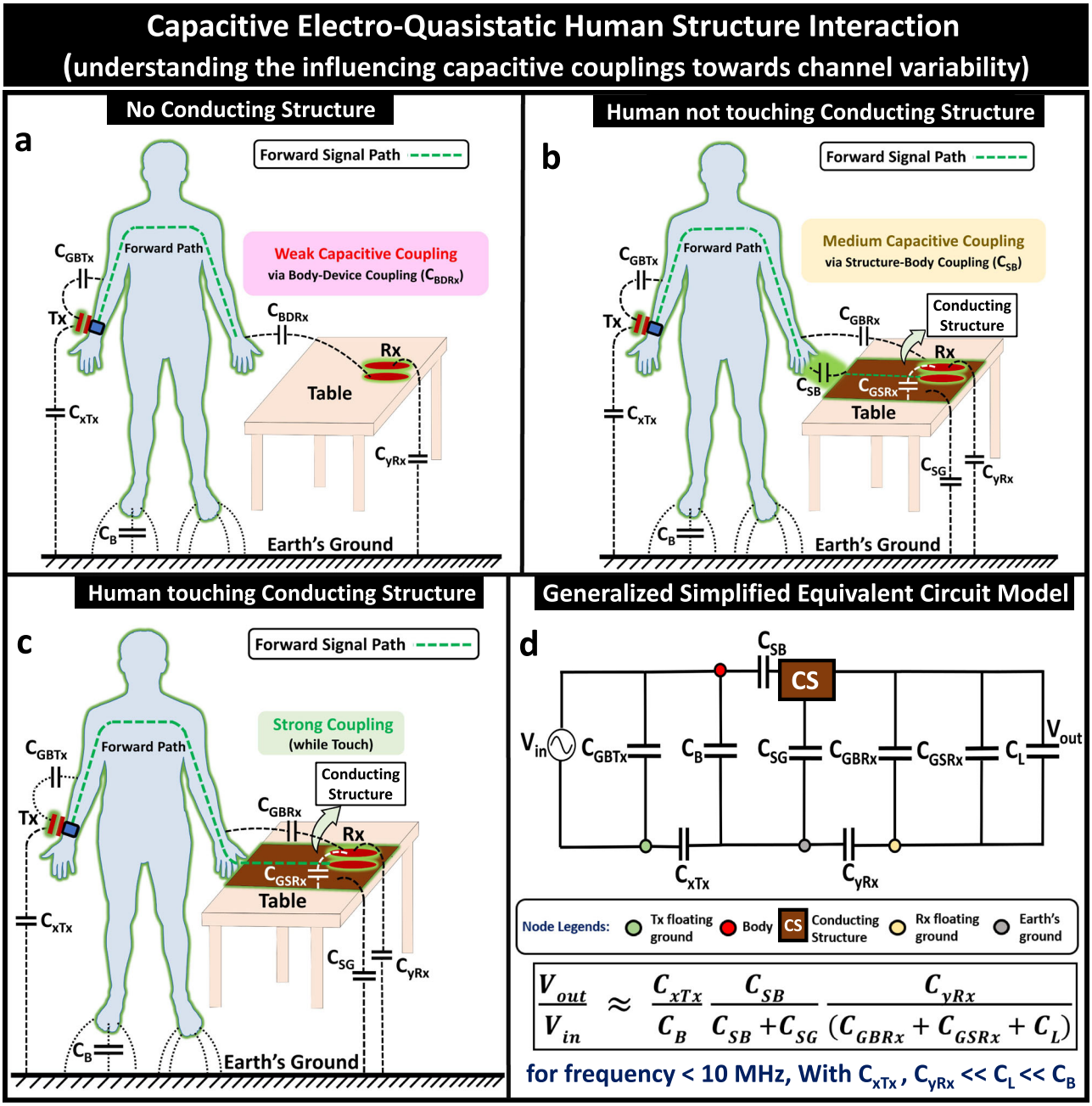

Fig. 2 | Analyzing electro-quasistatic human-structure interaction (EQS HSI). Schematic diagram illustrating involved capacitive couplings: with device's return path capacitances at the transmitter (Tx): C_{xTx}, at the receiver (Rx): C_{yRx}, the capacitance between device's floating ground and subject's body at Tx: C_{GBTx}, at Rx: C_{GBRx}, the capacitance between Rx-ground and conducting structure (CS) being C_{GSRx}, C_{SG} representing capacitance between CS and ground, subject's body capacitance being C_B, and C_L representing capacitive load at Rx, under different possible scenarios: **a** Non-guided communication: in the absence of conducting structure (CS), EQS field from the subject's body weakly couples to an off-body Rx, resulting in a reduced Body-to-Device coupling (C_{BDRx}). Introducing a CS as a guiding medium to improve the coupled E-field strength at Rx in EQS: **b** Human is not touching the CS: Medium capacitive coupling resulting from body-to-CS coupling (C_{SB}). **c** Human is touching the CS: Strong coupling resulting from touch-based interaction. **d** Generalized Simplified Equivalent Circuit Model and its transfer function.

received voltage (V_{Rx}) (in dBV) variations are calculated, and detailed descriptions of the EM simulation setups for the two modalities are delineated in the Methods section.

EQS HSI. This section depicts the effect of introducing a conducting structure (CS) as a guiding communication medium between objects involved in information exchange through capacitive coupling in the EQS regime. To gain physical insights into the contributing factors towards channel variability, the effect of the receiver's positional variation relative to the human body and body movement about the CS on channel transfer characteristics, are analyzed. The simulation setup, shown in Fig. 4a, emulates capacitive HSI with communicating devices of wearable form factor. In the absence of CS, the existing weak capacitive coupling (C_{BDRx}) between the body and Rx, based on their relative separation, decides the channel gain. The key differences between the guided (with CS) and non-guided (without CS) communication, are initially visualized through E-Field plots comparison in Fig. 4b, c and the extent of channel gain benefit with the guided mode is quantitatively summarized for different Rx-positions in Fig. 4e. In non-guided communication, the coupled signal strength remains lower (≤110 dBV).

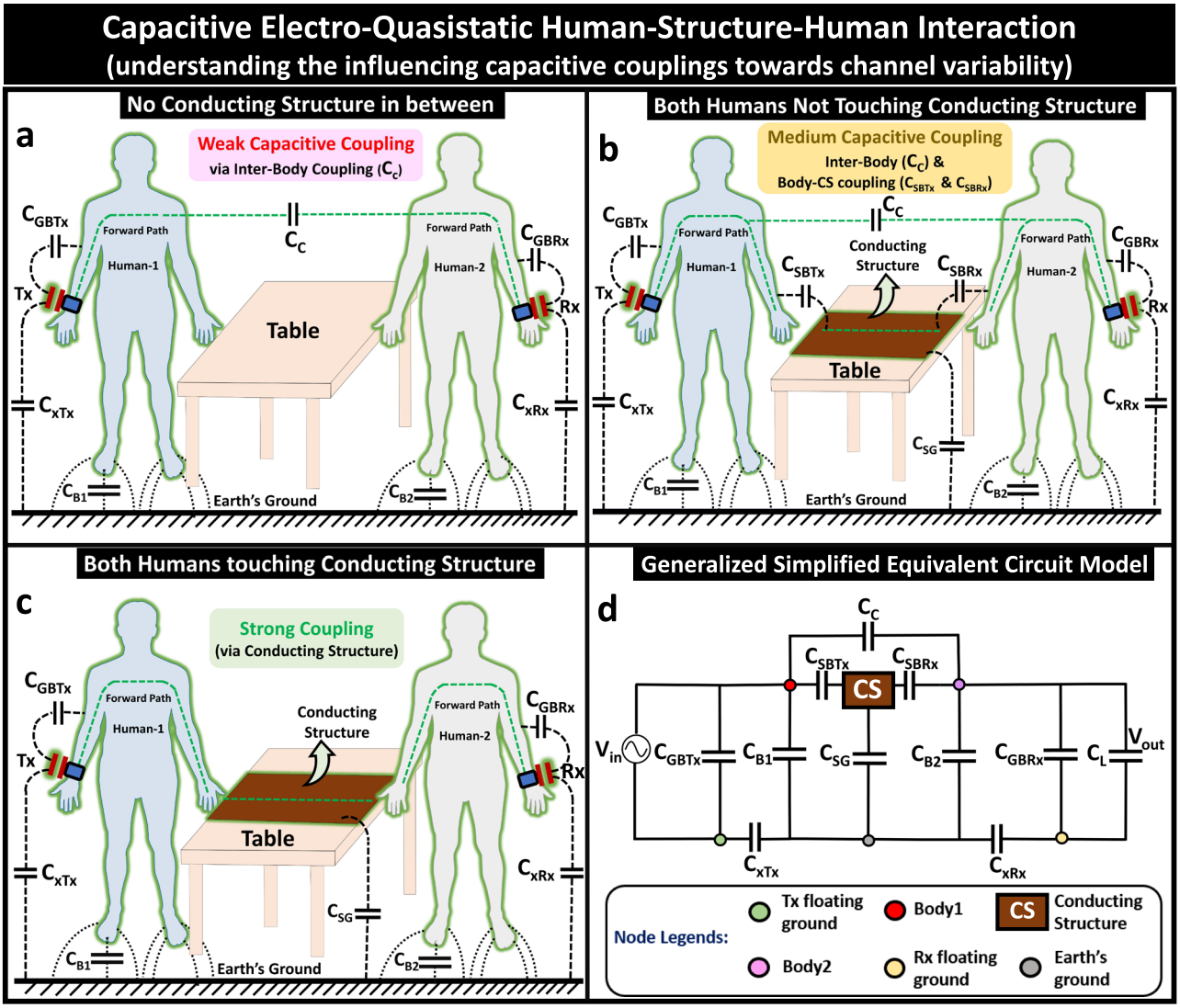

Fig. 3 | Studying human-structure-human interaction (HSHI). Schematic diagram depicting involved capacitive couplings with device's return path capacitances at the transmitter (Tx): C_{xTx}, at the receiver (Rx): C_{xRx}, capacitance between device's floating ground and subject's body at Tx: C_{GBTx}, at Rx: C_{GBRx}; C_{SG} representing capacitance between CS and ground, body capacitance of subject with Tx being C_{B1}, and with Rx being C_{B2}, and C_L representing capacitive load at Rx, under different possible scenarios. **a** non-guided communication: in the absence of CS, weak capacitive coupling between two subjects i.e., Inter-body coupling (C_C) decides the signal strength at Rx. Improving coupled signal strength by introducing a CS between two humans. **b** Humans are not touching the CS: medium capacitive coupling resulting from the inter-body (C_C) and body-to-CS coupling (C_{SBTx} and C_{SBRx}). **c** Touch-based interaction when both humans are touching the CS: strong coupling. **d** Generalized simplified equivalent circuit model.

However, it starts increasing as the Rx moves closer to the body on account of a rise in C_{BDRx}. On the contrary, the touch-based guided communication via CS with better signal confinement offers ~35 dB (56×) improvement in channel gain. Now, the received signal encounters a drop in its level as the Rx moves towards the body during touch-based interaction, which lies in the termination of more E-field lines on the CS and body (i.e., Body Shadowing[38]). This results in increase in C_{GSRx}, C_{GBRx} and a subsequent attenuation in C_{yRx}, as explained through the circuit diagram in Fig. 2d and its associated transfer function in Eq. (1) & (2)) and are confirmed through capacitance analyses obtained via numerical simulations in ANSYS Maxwell in Fig. 5f, g.

Towards understanding the distance beyond which capacitive coupling between body and CS becomes negligible and hence so as the EQS-communication, a limiting distance, namely critical distance (d_{cTx}), can be conceptualized. In the presence of the CS, for a fixed receiver position on the table, as the body starts moving away from CS, the reduction in the coupled EQS-field from the subject's body to the CS, results in an attenuation in body-to-structure coupling (C_{SB}) which leads to a decrease in voltage level at the Rx, delineated in Fig. 4d, f. The idea of this limiting distance appears to be independent of frequency in the EQS regime owing to the flat nature of the frequency response.

Factors contributing towards HSI channel variability. Besides the variation in voltage level with the distance between the body (with Tx) and CS (with Rx), the size (i.e., dimensions) and shape (i.e., patterning) of the CS, possesses a decisive influence on the received signal strength of the HSI link, shown in Fig. 5.

Dimensional variation of CS. Emphasizing the impact of sizing the guiding medium, a 100× reduction in CS's width results in a ~12 dB improvement in V_{Rx} at position B (5 cm away from the body) which increases to ~18 dB at position A (95 cm away from the body), shown in Fig. 5a, which can be visualized through E-field plot comparison, delineated in Fig. 5c. This rise in V_{Rx} is due to the reduction in C_{SG}, C_{GSRx} and an increase in C_{yRx}, illustrated in Fig. 5e–g. On the contrary, the variation in the length of the CS possesses minimal contribution towards deciding

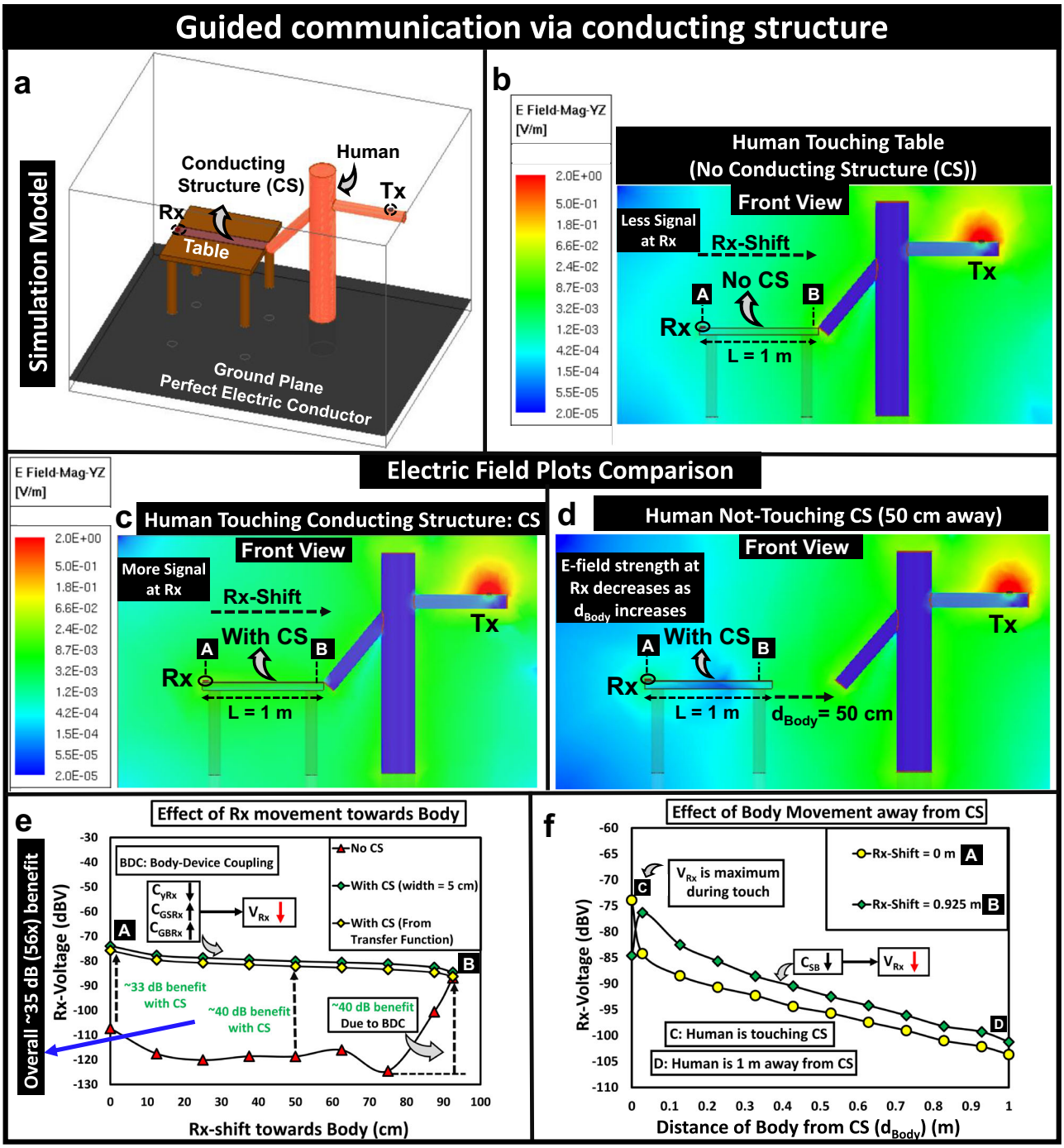

Fig. 4 | Simulation setup and results for human structure interaction. a Setup for numerical simulations, details are presented in Methods section. E-Field plots. **b** Without conducting structure (CS): weak coupling of Electro-Quasistatic (EQS) field from subject's body (with transmitter (Tx)) to an off-body receiver (Rx). **c** Strongly coupled touch-based interaction with CS as a guiding communication medium. Analyzing the limiting distance beyond which coupled EQS-field strength at Rx falls below its sensitivity: **d** Human is at 50 cm away from the CS. **e** Effect of Rx shift on the table towards body in presence and absence of CS. The Rx movement from the table-side towards subject's body leads to an attenuated Rx-Voltage (V_{Rx}) owing to an increase in couplings between CS-to-Rx ground (C_{GSRx}) and Body-to-Rx ground (C_{GBRx}), while a subsequent reduction in return path capacitance (C_{yRx}). **f** Effect of body movement away from CS during capacitively coupled interaction. As the subject moves away from the CS, with reduced structure-to-body coupling (C_{SB}), the received voltage goes down.

the extent of voltage pickup at the receiver, shown in Fig. 5b, i.e., V_{Rx} slightly goes down (~4 dB) with a 3× increase in length of CS owing to some increase in C_{SG}. The effect of change in structure-to-ground coupling (C_{SG}) with variation in CS's width for different lengths of CS, is captured in Fig. 5e. Now, to understand the distance-dependent channel variability between human and CS, the variation in structure-to-body coupling (C_{SB}) with the body movement away from CS, is presented in Fig. 5d.

Communication specificity via patterned CS. Patterning of the guiding medium can potentially offer specificity in communication by guiding EQS signals through the conducting structure at intended locations during touch-based interaction, as shown in Fig. 6.

Conducting square rim & cross-shaped patterned structure. In view of increasing the signal strength around the edges of a conference room table, when the CS is patterned like a square rim (width = 5 cm) as shown

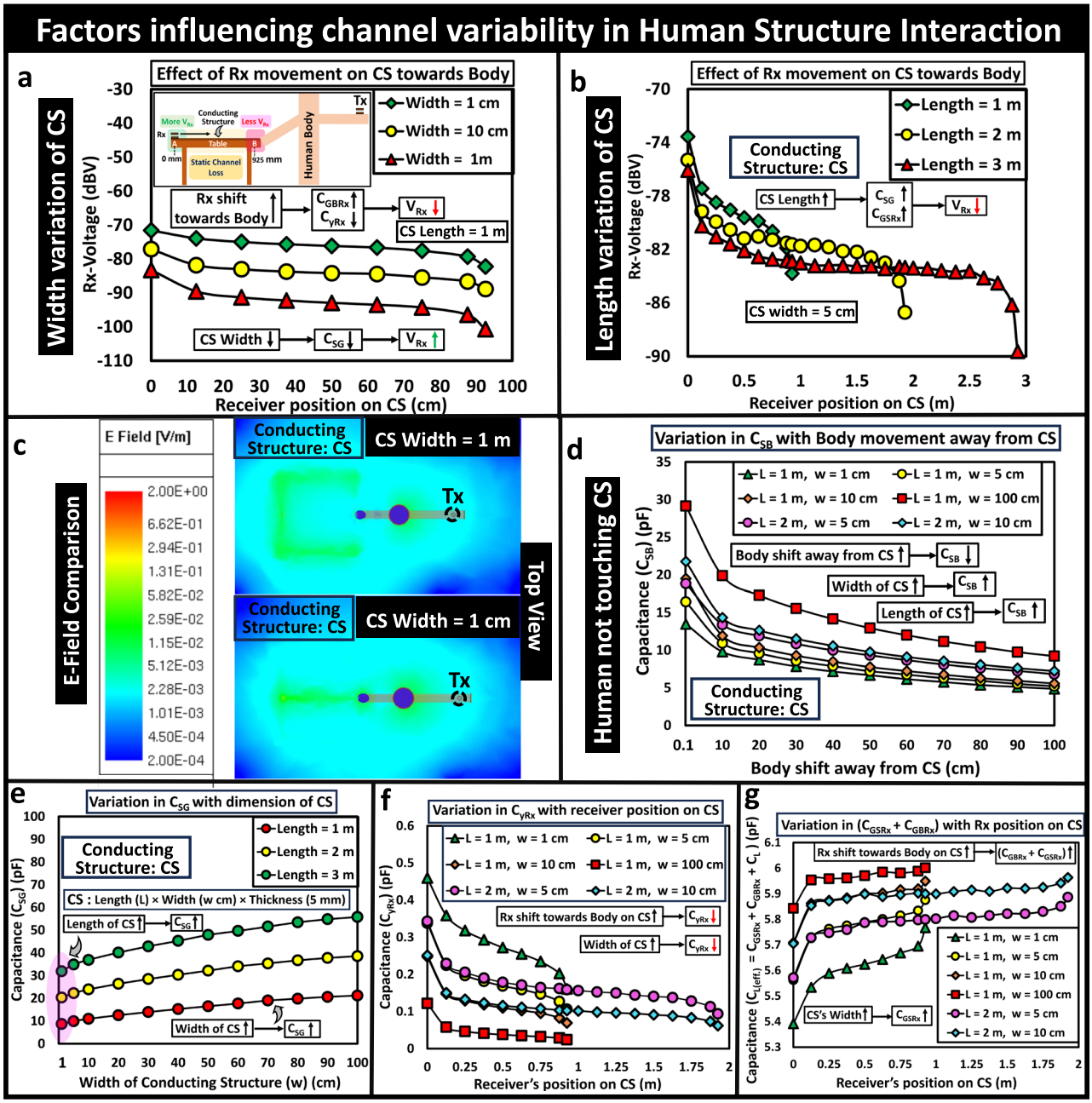

Fig. 5 | Contributing factors towards channel gain variation: conducting structure (CS) dimension (length (*L*) × width (*w*) × thickness (*t*)). **a** Width (w) variation: higher received voltage (V_{Rx}) with reduction in width of CS, due to an attenuation in CS-to-Rx-ground coupling (C_{GSRx}) and a subsequent rise in return path capacitance (C_{yRx}). **b** Length (L) variation: minimal variation in channel gain with increase in the length of CS. E-field Plots Comparison. **c** Width = 1 m and 1 cm to support the proposed hypothesis. Analysis of the variations in corresponding coupling capacitances. **d** Change in Body-to-Structure coupling (C_{SB}) with body movement away from CS for different widths (w) and lengths (L) of the structure. **e** Structure-to-ground coupling (C_{SG}) changes with width of CS for different lengths. **f** Variations in receiver's return-path capacitance (C_{yRx}) with receiver's position on CS. **g** Change in receiver's floating ground-to-(CS and Body) coupling ($C_{GSRx} + C_{GBRx}$) with receiver movement towards body.

in Fig. 6a, an ~16 dB attenuation in V_{Rx} is experienced with receiver movement towards the body along the edge A-O_1-Body-O_2-B (where the human is touching) as shown in Fig. 6c, due to an increase in C_{GBRx}. However, Rx movement along the non-touching edges (i.e., AD, BC, and CD) doesn't offer noticeable variation except at the corners due to the availability of the E-field lines of the receiver ground to terminate directly to the earth's ground leading towards higher C_{yRx}. Similarly, aiming to maximize V_{Rx} at the corners of the table, when the CS is patterned similar to a cross-shape as shown in Fig. 6d, an increase in E-field strength at the corners is observed as pictured in Fig. 6e. Similar to the square rim, this increased field strength can be attributed to an increase in C_{yRx} with a subsequent decrease in C_{GSRx}. However, moving the receiver from the corners to the center of the Cross-shaped CS results in a ~12 dB attenuation in V_{Rx} owing to an increase in C_{GSRx} at the expense of a reduction in C_{yRx}, illustrated in Fig. 6f.

EQS human-structure-human interaction. The simulation setup for capacitive human-structure-human interaction in the EQS regime is presented in Fig. 7a. The results from numerical simulations for HSHI can be analyzed as follows: In case of non-guided communication between two humans, inter-body coupling[21], which depends on subject relative orientation and separation, primarily decides the channel

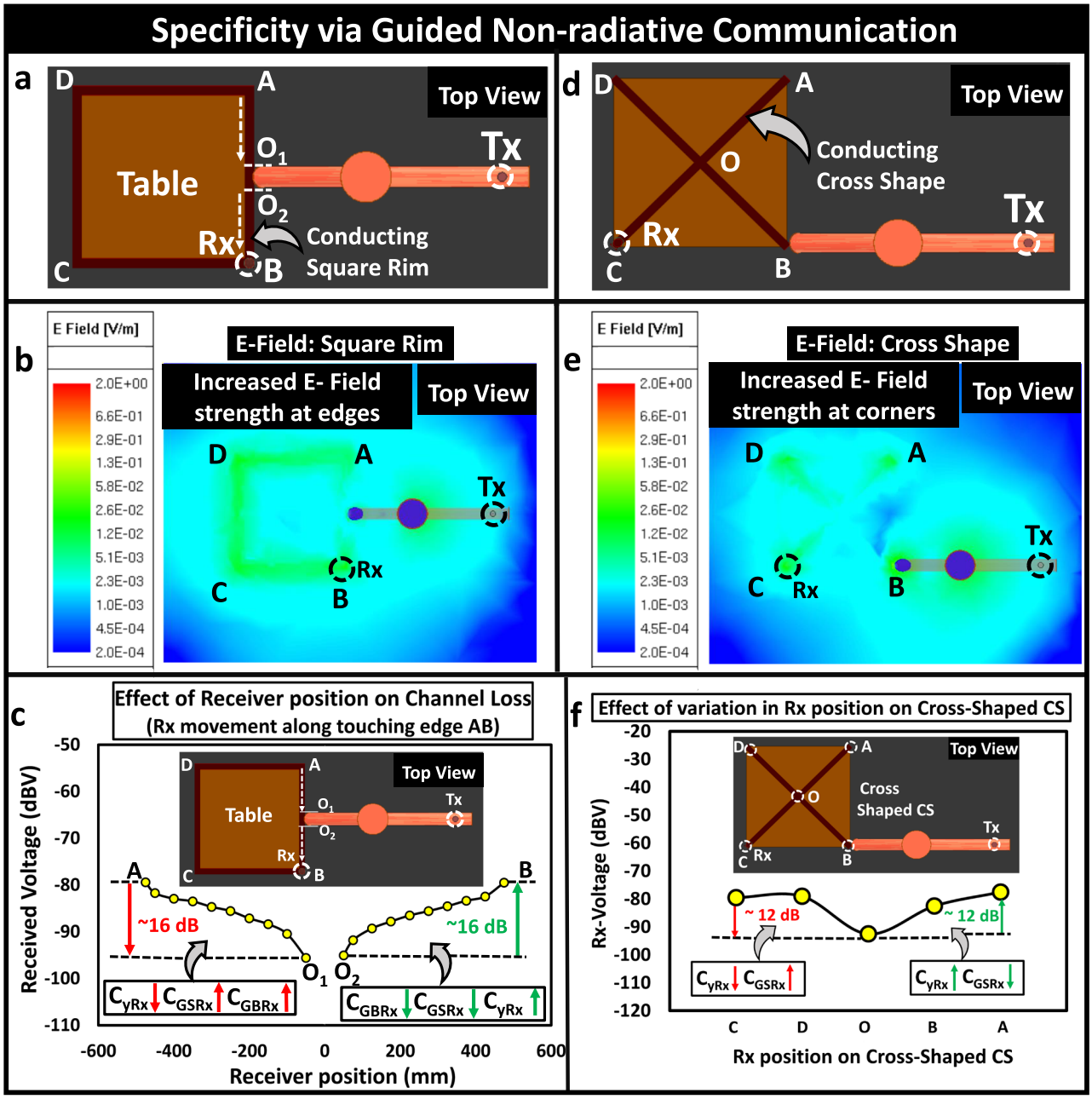

Fig. 6 | Specificity though guided non-radiative communication: need for application-specific pattering of conducting structure (CS). Conducting square rim: **a** top-view of the simulation setup. **b** Electric field distribution while human is touching the edge AB of the Square Rim. **c** The effect of receiver's (Rx) positional variation along the touching edge AB of CS. Received signal strength (V_{Rx}) goes down with an increase in CS-to-Rx ground coupling (C_{GSRx}) and Rx ground-to-body coupling (C_{GBRx}) while a consequent reduction in return path capacitance (C_{yRx}) as the Rx moves away from the CS's corners towards subject's body and vice-versa. Conducting cross shape. **d** Top-view of the simulation setup. **e** E-Field distribution while human is touching the corner B. **f** The effect of variation in receiver position on the cross-shaped CS.

characteristic as depicted in Fig. 7b. Strengthening of the coupled EQS field around the subject's body ensures wireline-like benefits during touch-based interactions, represented in Fig. 7c. This guided mode of inter-human interaction during touch offers ~25 dB improvement in channel gain than its non-guided counterpart, depicted in Fig. 7e. The trends of change in return-path capacitances (i.e., C_{xTx} and C_{xRx}), at the transmitting and receiving end with a positional variation of Tx & Rx on the subject's arm, are found to be concurrent as proposed previously[38]. Similar to the idea of critical distance from the transmitting end (d_{cTx}) as mentioned previously for HSI, its notion can also be extended for HSHI at the receiving end. When the subject with the receiver, starts moving away from the CS, the E-field strength around the subject's body reduces, resulting in an attenuation in C_{SBRx}, shown in Fig. 7d. The effect of body movement with a receiver away from the CS is appreciated in Fig. 7d. Thus, from the idea of critical distance from receiving end (d_{cRx}) for HSHI, d_{cRx} remains ~10 cm.

Experimental results

To validate the observed trends in numerical simulation results, channel gain measurements are performed in a conference room environment. We use a wearable capacitive transmitter and a handheld portable spectrum analyzer as receiver to emulate measurements with battery-powered miniaturized wearable devices. The experiments are conducted at 1.53 MHz, details are comprehensively described in the Methods section under the

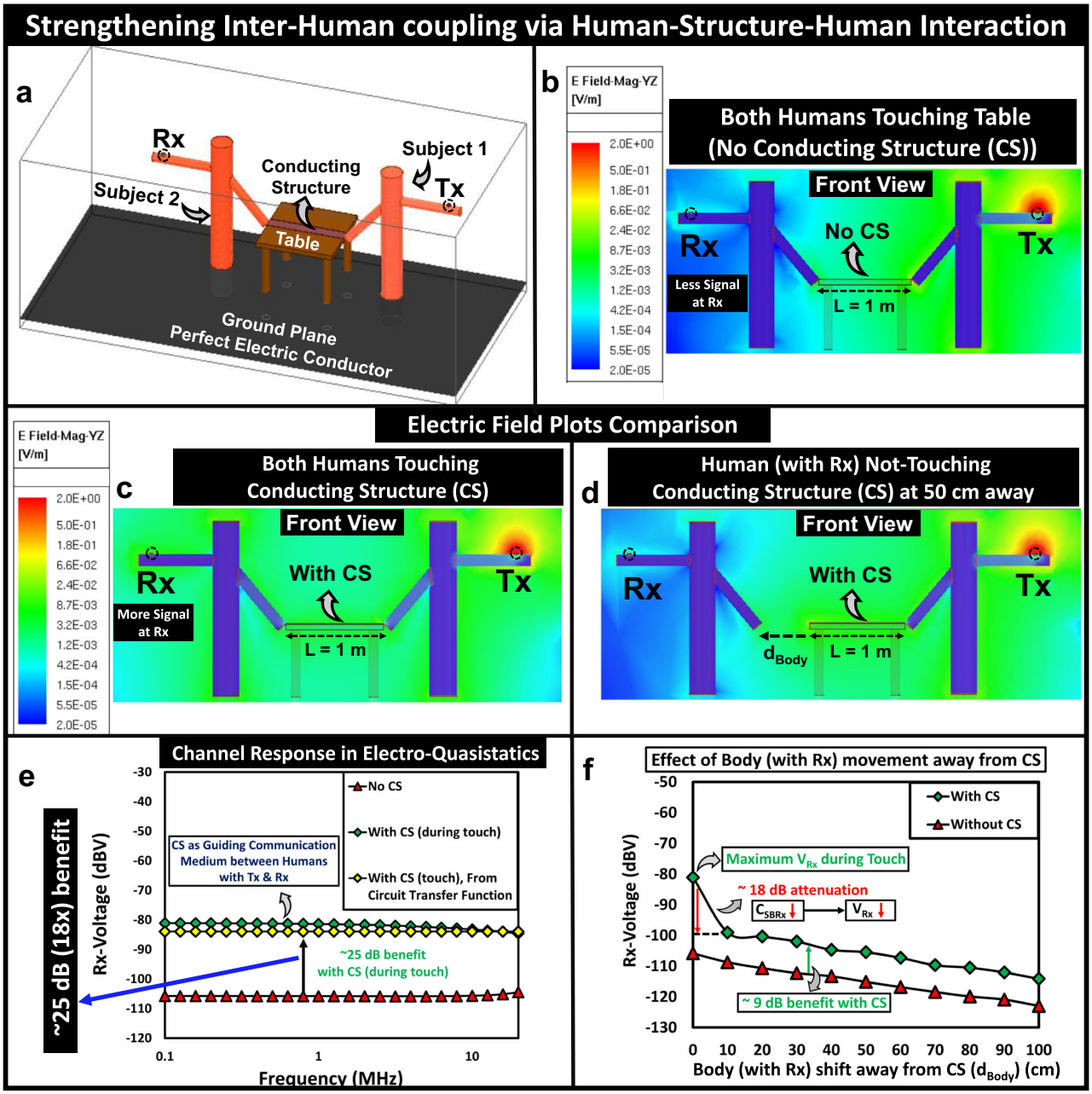

Fig. 7 | Simulation setup and results for human-structure-human interaction (HSHI). a Setup, details are described in Methods section under the subsection namely Setup for EQS Simulations. E-field plots comparison. **b** In absence of conducting structure (CS), the two subjects weakly couple to each other via inter-body coupling (C_C). **c** Touch-based interaction when both humans are touching the CS, offers strongest coupling. Extending the similar idea for limiting distance i.e., distance beyond which the coupled EQS signal strength falls below the Rx-sensitivity: **d** Received signal strength goes down as the human with receiver removes touch and starts moving away from CS. **e** HSHI Channel characteristics in EQS-Regime: benefits of guided communication in capacitive inter-human interactions. **f** Effect of movement of body with receiver away from CS: with reduction in structure-to-body coupling (C_{SBRx}), received signal (V_{Rx}) attenuates, i.e., touch-based interaction offers maximum channel gain owing to the strongest coupled field strength at Rx.

subsection Experimental Setup. The reason for the measured channel gain to vary from the simulations lies in the presence of additional ground planes (increase in the return-path capacitance, i.e., C_{xTx} and C_{xRx}) in the measuring environment and differing ground sizes of the communicating devices. However, we confirmed the trends of channel gain variability to match as observed in simulations through repeatability in measurement readings.

The measurement results of capacitive EQS-HSI, presented in Fig. 8a, capture the channel gain dependency on the positional variation of Rx relative to the human body during touch-based interaction. The movement of Rx on CS towards the body leads to an attenuation in the received signal (V_{Rx}) owing to the body shadowing as perceived through simulation results in Fig. 4e. Conforming the simulation results as depicted previously in Fig. 6, reducing the width of the CS during measurements showed an increase in V_{Rx} due to an increased coupling from CS to the earth's ground. The channel gain variation with Rx movement on a patterned square-shaped CS, presented in Fig. 8b, c, corroborates the previously observed trends through FEM-based simulation results in Fig. 6. While the human (with Tx at the non-touching arm) is touching the CS at a position O as indicated in Fig. 8b, the receiver's movement along the segment AO_1 of the touching edge AB towards the arm causes the V_{Rx} to go down due to body shadowing. The maximum V_{Rx} is experienced at the corner positions (A & B) of the

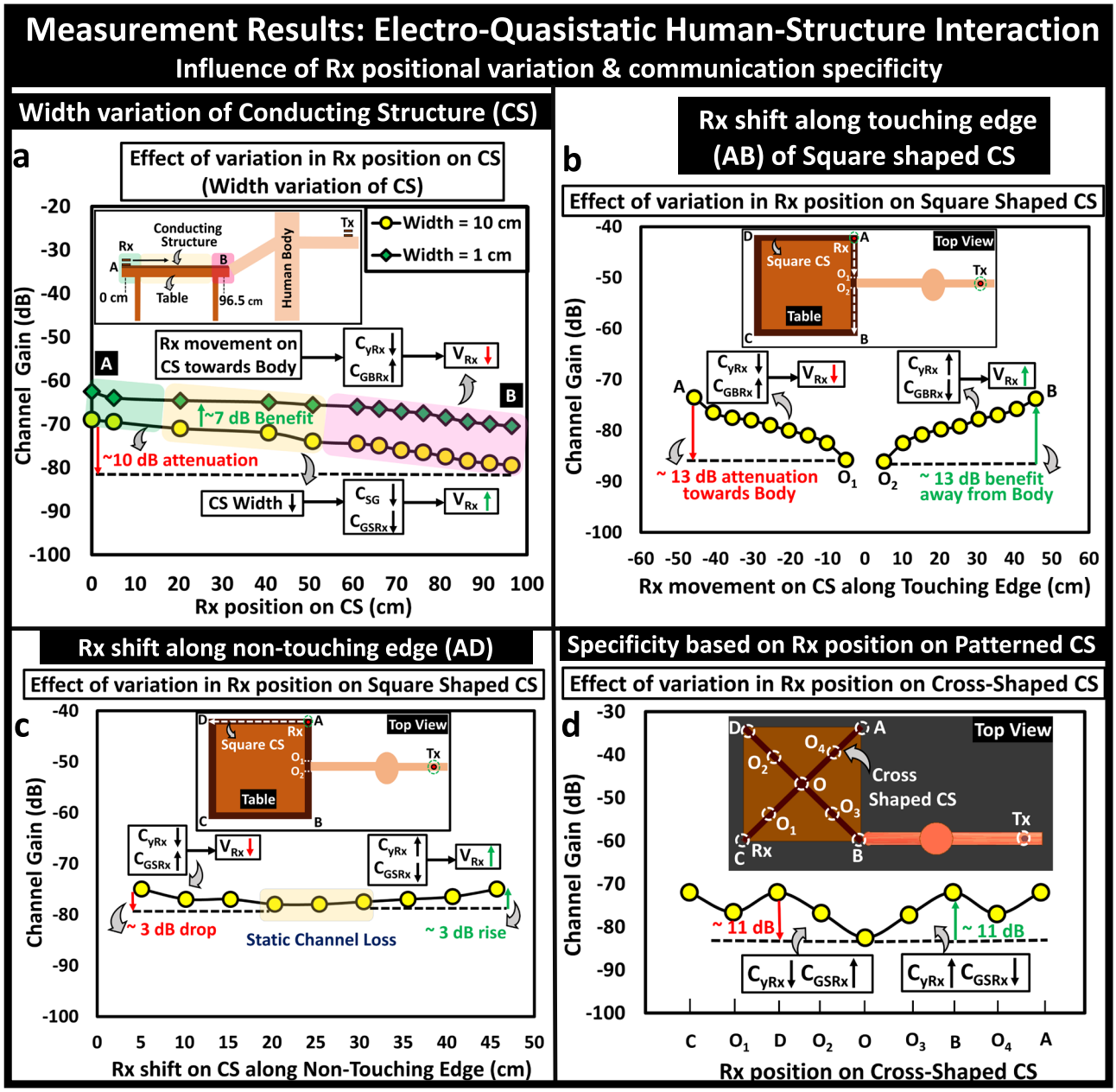

Fig. 8 | Measurement results. Human-structure interaction. **a** Movement of receiver (Rx) on the conducting structure (CS) towards subject's body for different widths of the structure. Increase in CS's width leads to an increase in CS-to-ground coupling (C_{SG}) and the coupling between CS-to-Rx ground (C_{GSRx}), and thereby reduces the signal strength at Rx (V_{Rx}). Besides, the movement of Rx towards subject results in an attenuation in the return path capacitance (C_{yRx}) from an increase in the coupling between Rx-ground-to-subject's body (C_{GBRx}). **b** Movement of Rx on square-shaped CS along touching edge (AB). **c** Movement of Rx on square-shaped CS along the non-touching edge (AD & BC). **d** Movement of Rx on cross-shaped CS influencing channel gain.

patterned CS because of the lowering of the shadowing of E-field lines from Rx-ground by CS. The receiver's movement along the non-touching edges (i.e., along AD) of the square-rim doesn't offer appreciable variation in channel gain except at the corners, illustrated in Fig. 8c. Aiming to enhance the communication specificity only at the corners of a square-shaped table, when the CS is patterned like a cross-shape as shown in Fig. 8d, lower shadowing (i.e., C_{GSRx}) at the corners ensures maximum voltage pickup while the received signal level at the center O gets affected due to higher shadowing of the field lines of the Rx-ground from the CS.

Influence of touch & leakage analysis in EQS HSI

To confirm the non-radiative guided nature of the proposed on-body-to-off-body link, the results from the numerical simulations and experiments are illustrated below: (i) The proposed modality, being non-radiative, guides the EQS signals through the human body and the employed CS that provides a well-defined pathway for signal transmission and offers specificity through touch-based interactions. The results from numerical simulations and experiments, portrayed in Fig. 9a, b, highlight the benefits of touch-based interaction. The attenuation in channel gain (~12–15 dB) during a non-touching scenario with the user's hand 1 cm above the CS effectively proves the non-radiative nature of the communication link. (ii) Furthermore, being non-radiative, the introduced modality offers lower leakage (i.e., ~10X more received signal when the receiver resides on the CS than the scenario when the receiver is 5 cm away from the CS), as delineated in the simulation and experimental results, presented in Fig. 9c, d, which emphasizes the physical security aspects of the introduced communication link. A comparison of the proposed non-radiative interaction modality with traditional radiative wireless communication is presented in Supplementary

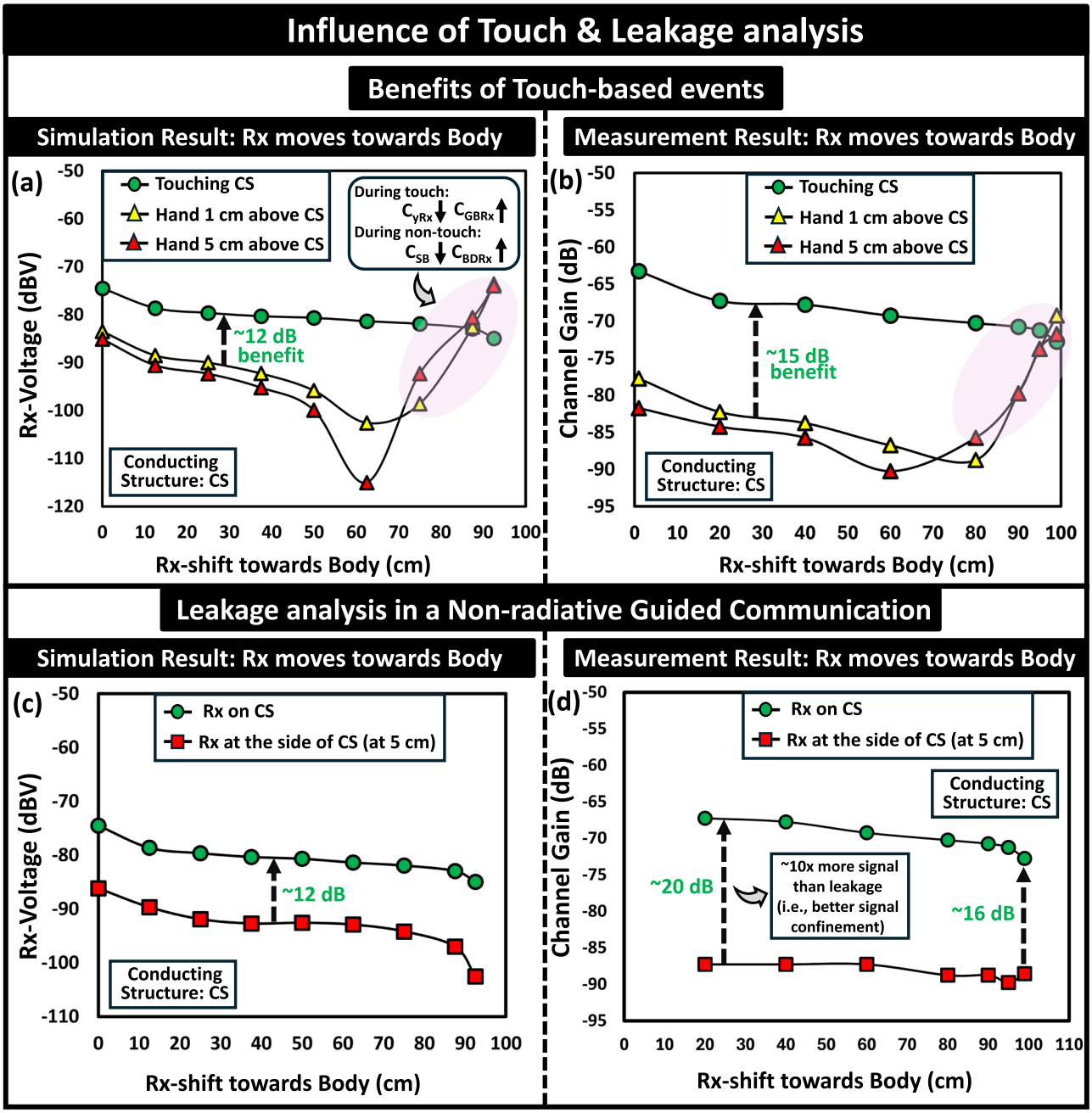

Fig. 9 | Influence of touch in human structure interaction. Received voltage variation with receiver (Rx) movement relative to subject's body under different scenarios of human interaction with conducting structure (CS). **a** Simulation result, **b** Measurement result. Touch-based communication offering benefit in channel gain in comparison to non-touching scenarios which incurs reduced structure-to-body coupling (C_{SB}). **Analysis of leakage in the proposed non-radiative guided communication**: **c** Result from numerical simulation. **d** Result from measurements. Considerably lower leakage even at relatively shorter distance (~5 cm) depicts the non-radiative nature and hence physical security aspects of the proposed communication link.

Fig. 1 in the Supplementary Information. The protocol level or mathematical security from encryption can always be augmented on top of the illustrated physical security benefits of the introduced modality, achieved through the confinement of the EQS signal, to enable several secured HSI applications.

Intending to enable the touch-based guided mode of inter-human interaction in EQS, the results from the HSHI channel measurements are delineated in Fig. 10, where Fig. 10a, b illustrate the scenarios with the communicating devices (Tx & Rx) on the human arms that are not touching the CS. The effect of variation in the body position for the human (with Tx) relative to the CS, as shown in Fig. 10a, depicts that a decrease in body-to-structure coupling at the transmitting end (C_{SBTx}) results in a sharp reduction in voltage level at the Rx (i.e., ~18 dB attenuation as the human with Tx moves 5 cm away from the CS) which proves the touch-based communication is energy-efficient. Beyond 10 cm, the measured signal level falls below the noise floor of the receiver. Similar trends of variation in V_{Rx} with the change in body position of the human (with receiver) relative to CS are experienced due to the reduction in C_{SBRx}, shown in Fig. 10b.

Though seemingly a wired medium with potential complexity in installation, the proposed technique leverages the conducting parts of already existing structures around us like a table or a chair with metal legs, doors, car chassis, and any other objects with metallic parts at home or office places, to enable an on-body-to-off-body link with flexibility in deployment distance (i.e., suitable for both short and long-distance communication) by

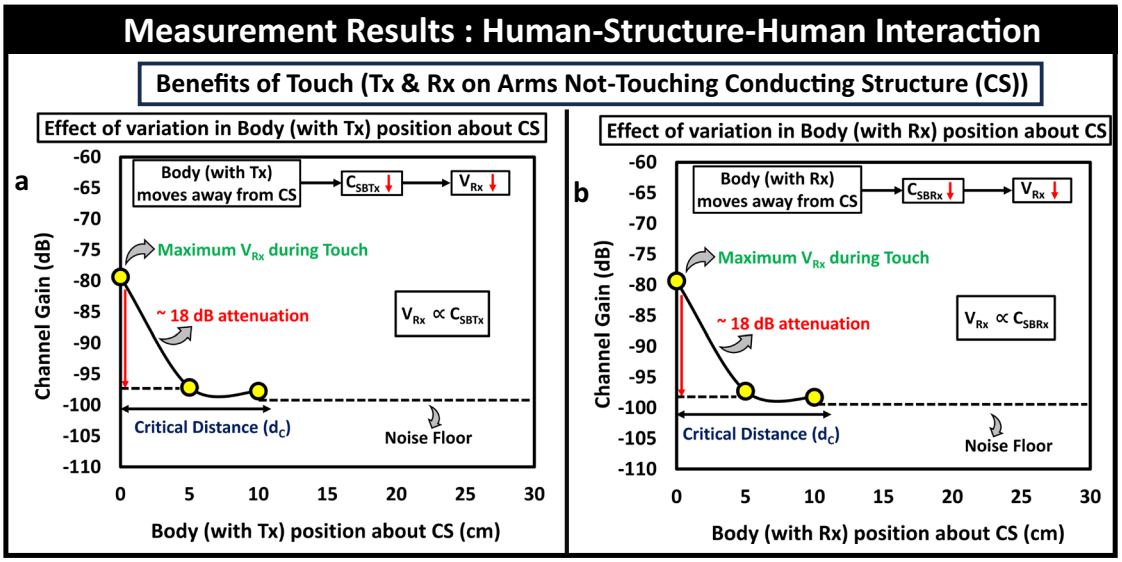

Fig. 10 | Measurement results for human-structure-human interaction. Benefits of touch-based interactions: Humans with wearable transmitter (Tx) & receiver (Rx) in their arms not-touching the conducting structure (CS). **a** Movement of the subject (with Tx) away from CS, resulting in an attenuation in the subject's body-to-CS coupling (C_{SBTx}) that leads to a reduced received voltage ($V_{Rx} \propto C_{SBTx}$). **b** Movement of the subject (with Rx) away from CS, causing an attenuation V_{Rx} from the reduced C_{SBRx}, since $V_{Rx} \propto C_{SBRx}$. Sharper attenuation in channel gain characteristic as the human with communicating devices removes touch from CS, confirming non-radiative energy-efficient touch-based communication.

Fig. 11 | The impact of electro-quasistatic human structure interaction link in practical scenario. Demonstration of real-time audio signal transfer via human body communication (HBC) and the proposed human-structure interaction (HSI). Schematic Diagram, representing signal flow from a wearable transmitter (Tx) through the human body and conducting structure (CS) to an off-body wearable receiver (Rx), placed on the CS. Complete demo setup is illustrated in Fig. 1d.

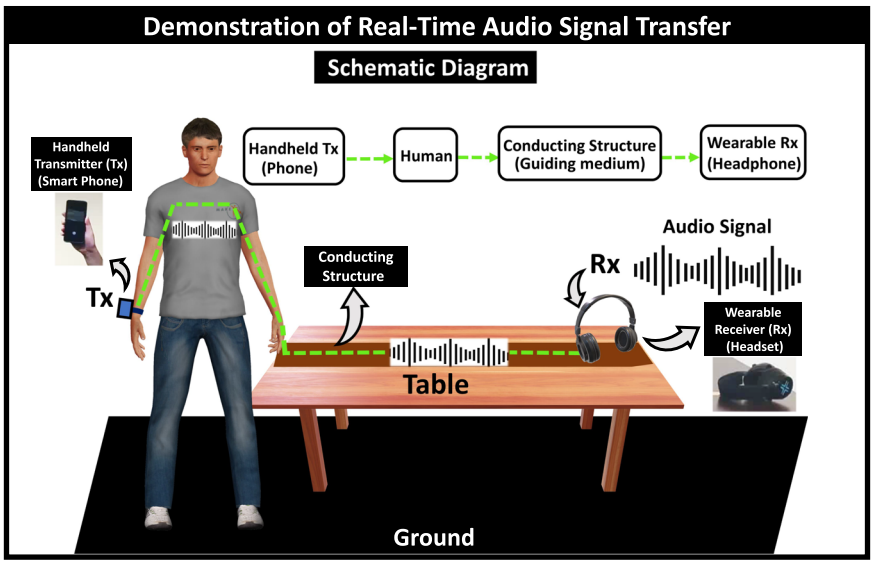

guiding EQS signals to the intended locations through touch, while offering wireline-like benefits that can inspire the development of many energy-efficient HMI applications.

Demonstration of audio streaming

This section presents an application of the proposed capacitive-coupling-based EQS HBC-HSI link by demonstrating the real-time transmission of an audio signal from an on-body transmitter (i.e., smartphone) through the human body and a conducting structure and successful reception to an off-body receiver (i.e., wearable headset). The demonstrated audio streaming exemplifies the feasibility of data transfer at 1.44 Mbps over an on-body-to-off-body communication link using battery-powered wearable form factor devices. The mode of communication, being digital, with a low bit-error rate (BER < 10^{-3}), ensures reliable transfer of the digital data packets while maintaining the quality of the audio transmission. The schematic for the demonstration is shown in Fig. 11. The details of the demonstration setup are included in Supplementary Discussion 2, with this paper, illustrated in Supplementary Fig. 2 and Supplementary Fig. 3, and the demo video has been provided as a Supplementary Movie file.

Conclusion

In this paper, we propose two fundamental modalities for non-radiative touch-based communication between humans with wearables and surrounding electronic devices, namely HSI and HSHI in EQS regime while enabling off-body links that support communication specificity via guided communication. Besides offering better signal confinement over non-guided radiative interactions, the reason for choosing the operating frequency in the EQS regime ($f \leq 10$ MHz) lies in minimizing the following: radiation in the surroundings to increase the communication specificity during touch and power consumption at the transmitting end to make the

link energy-efficient. Proposed touch-based guided interactions, with selectivity in communication, can offer a ~35 dB (56x) benefit in end-to-end channel gain for HSI, which becomes ~25 dB (18x) for HSHI. Subsequently, highlighting the profound impact of the work in practical scenarios, we demonstrate a real-time transmission and reception of an audio signal through the HBC-HSI link in the EQS regime. Finally, we envision that combining EQS-HBC with the proposed HSI can facilitate emerging technologies to drive the domain of HMI.

Methods

This section deals with the details associated to our simulation and experimental methods, to facilitate reproduction of results by any researcher in future.

Setup for EQS simulations

EQS simulations are executed using ANSYS HFSS, which performs finite element method (FEM) based solutions for Maxwell's Equations. A simplified cross-cylindrical model for the human body has been used to reduce computational time and complexity for FEM-based simulations, shown in Fig. 12, whose accuracy was previously validated[23] through comparison of its field distributions and the currents in and around the human body with a detailed model. Dielectric properties (i.e., relative permittivity (ϵ_r) and conductivity (σ)) of skin and muscle tissues have been adopted from the works of Gabriel et al.[46].

Simplified human body model. A simplified model using two perpendicular cylinders of height 180 cm with radius 14 cm and 6 cm representing torso and extended arms respectively, is created, shown in Fig. 12. Torso and arms are considered to be divided into an outer shell of skin of thickness 4 mm and an interior muscle. One arm of the cross-cylindrical model has been rotated at 50° to mimic the touch-based interaction, as shown in Fig. 12 b. In simulation, we assumed this human body model is 40 cm above a plane with Perfect E Boundary in HFSS to emulate an infinite ground plane or the earth's ground.

Conducting structure with supporting table. A conducting structure (CS) made up of copper (relative permittivity (ϵ_r) of 1 and bulk conductivity (σ) of 5.8×10^7 S/m), measuring 100 cm × 5 cm × 0.5 cm, is used to serve the functionality of a guided communication medium. To support it well above the perfect E plane, it is mounted on a four-legged wooden table made up of plywood with ϵ_r of 8.13 and σ of 9.12×10^{-7} S/m. The square-shaped table-top, measuring 100 cm × 100 cm × 6 cm, is kept 109 cm above the reference perfect E plane.

The complete model is enclosed in an air region to act as a radiation boundary for the simulation setup with dimensions as follows: 280 cm × 400 cm × 280 (for HSI), 280 cm × 600 cm × 280 cm (for HSHI). Details of the excitation to the simulation model is provided through capacitive coupling as depicted in the subsequent subsections.

Excitation. A capacitive coupling model with the signal electrode connected to body while ground electrode kept floating, is used to provide excitation to the body, illustrated in Fig. 12e. Two copper discs of radius 2.5 cm are employed to function as signal and ground electrodes of the transmitter. One of the discs with 2 mm thickness is curved onto the arm to emulate the signal patch while the ground electrode of an wearable watch-like HBC device has been recreated using the other disc with 5 mm thickness. The separation between the signal and ground plates is kept at 5 mm. Aiming to replicate the functionality of an ideal AC voltage source with alternating potential difference of amplitude 1 V, in HFSS a voltage source excitation is placed in between the signal and ground plates. The assigned voltage source together with its signal and ground plates constitutes the transmitter (Tx) setup for HSI and HSHI.

Voltage measurement at the receiver. Two parallel discs of the following dimensions: cylinders with radius of 2.5 cm and thickness of 5 mm and are separated by 5 mm, have been used at the receiving end, making it structurally similar to that of the transmitter. Instead of placing a separate lumped RLC boundary, between the electrodes, the existing parallel plate capacitance between the two plates is employed for capacitive high impedance termination at the receiving end. The potential difference between the signal and ground plates is calculated by integrating the electric field along a straight line between the electrode and ground plates. For HSI, the receiver's (Rx) signal plate is placed on the CS, presented in Fig. 12f, whereas it remains in contact with the user's body as a wearable for HSHI, shown in Fig. 12g. With the amplitude or peak of the input excitation being 1 V, the presented simulation results for Rx-Voltage, expressed in dBV, is comparable to the channel gain measurements.

Calculation of coupling capacitances in proposed model. The coupling capacitances that are theoretically postulated in the bio-physical model, are calculated using ANSYS Maxwell, a FEM-based static Maxwell's Equations solver. In the electrostatic mode of simulation in Maxwell, by considering the two bodies as conducting objects from the computed capacitance matrix, the capacitance between the two objects is evaluated.

Experimental setup

Experiments are conducted in a standard conference room environment to replicate the real-world scenarios in a web-enabled smart conference room. The experimental protocols involving human subjects have been approved by the Purdue Institutional Review Board (IRB Protocol 1610018370). All guidelines and regulations, as given by the Purdue IRB were followed during the experiments. Informed consent was obtained from all the participants for the experiments. To obtain realistic channel gain measurements, a wearable transmitter and tiny SA spectrum analyzer are used in contrast to a wall-connected Vector Network Analyzer, which offers an optimistic estimation of channel transfer characteristics. The subject's body posture, transmitter and receiver devices used, and the overall system schematic are shown in Fig. 13.

Transmitting device. A PCB with an embedded ARM cortex microcontroller unit (MCU): NXP LPC55S69, is customized to perform the function of a transmitter (Tx) in EQS regime, shown in Fig. 13b. Being an wearable transmitter, it is housed in a 3D-printed enclosure, and powered up by a small 3.7 V rechargeable lipo battery. Functionality of the couplers at the Tx-end is emulated by fixing a copper tape to the surface of the Tx setup, which remains in contact with the skin. Electrical connection is made between the coupler and one of the GPIO pins of the MCU which is programmed to generate 3.3 V (peak-peak) excitation at a frequency of 1.53 MHz.

Conducting structure with supporting table. A commercially available double-sided conductive copper foil tape, measuring 1 m in length, 5 cm in width, and of <1 mm thickness is used to function as a conducting structure, illustrated in Fig. 13a. A four-legged wooden table with a square-shaped table-top, measuring 1 m in length and 1 m in width, is used to support the conducting structure at a height of 90 cm above the ground.

Receiving device: spectrum analyzer and buffer. A spectrum analyzer (tinySA basic) of wearable form factor is used as a receiver (Rx), shown in Fig. 13c. Functionality of voltage mode coupler (i.e., signal electrode) to the body at the Rx end is emulated by a copper tape, fixed at the bottom of the spectrum analyzer. The positioning of receiver is subjected to change during the two communication modalities, i.e., the receiver is placed above the conducting structure for human-structure interaction while it is kept on the body of a second human during Human-Structure-Human interaction. This device with its 50 Ω input impedance offers 50 Ω resistive termination.

Voltage mode communication with capacitive termination. Though the employed tiny SA spectrum analyzer, with its 50 Ω input impedance, measures the output power (in dBm) while being used as a receiver, we have incorporated a buffer in-line before the spectrum analyzer to

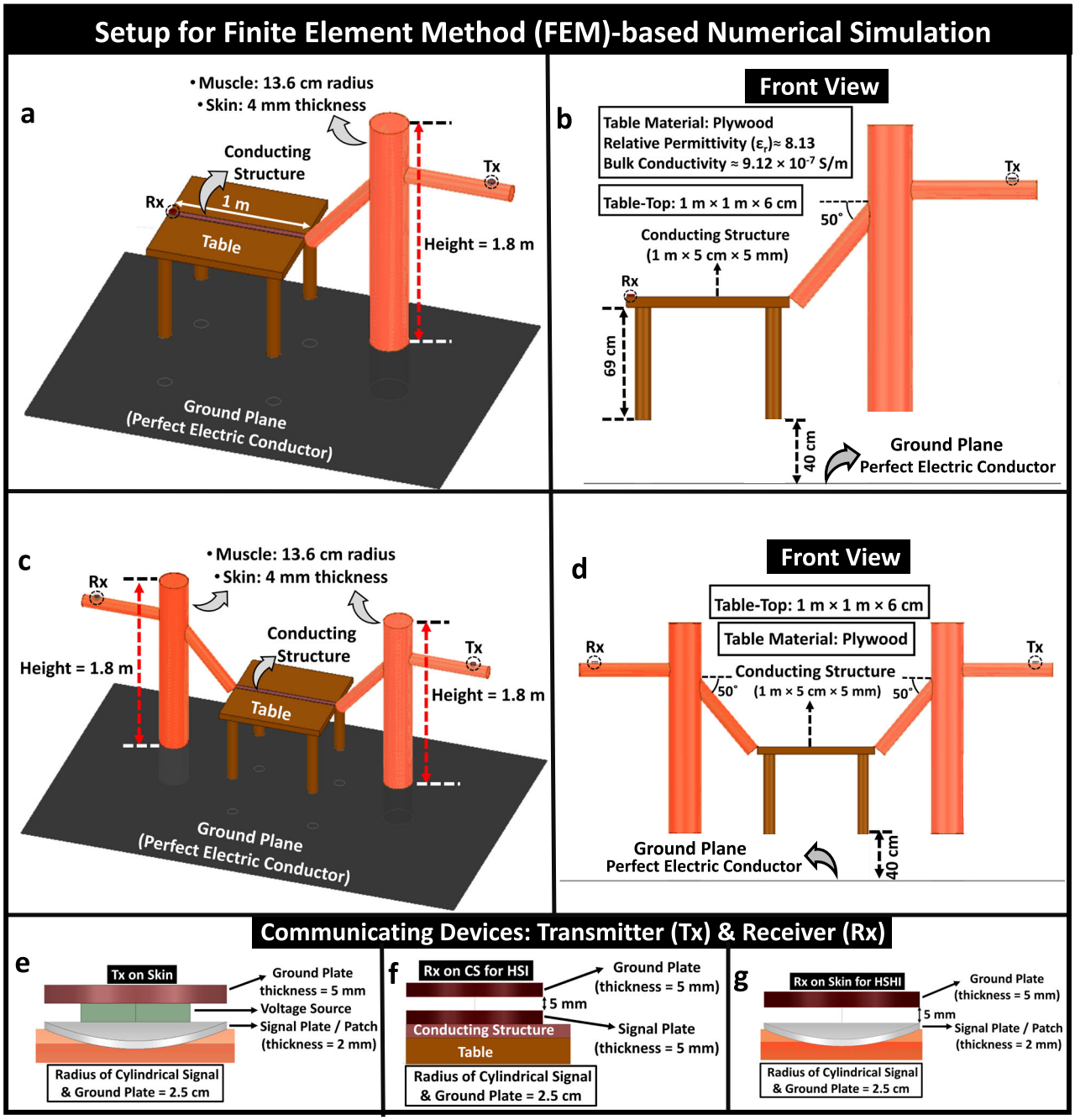

Fig. 12 | Finite element method (FEM)-based numerical simulation setup for the two proposed modes of interaction: human-structure interaction (HSI). **a** Simulation setup with model dimensions. **b** Front view of the setup, human-structure-human interaction (HSHI). **c** Simulation Setup with model dimensions. **d** Front view of the setup, communicating devices. **e** Wearable transmitter (Tx) used for HSI and HSHI simulations. **f** Receiver (Rx) (wearable form factor) used for HSI simulations. **g** Receiver (wearable form factor) used for HSHI simulations.

measure its corresponding voltage. Now, from an energy consumption perspective, one may wonder why the measurement of received power has more energy i.e., assuming an iso-voltage reception, the 50 Ω system has more energy compared to a high impedance system ($\frac{V^2}{R} >> \frac{V^2}{Z}$), the reasons in support for the use of voltage mode communication emerges from the following facts: (i) An iso-voltage reception is not possible for EQS-HSI channel with a lower Z for a given Tx voltage, as can be seen from the simplified equivalent circuit model, shown in Fig. 3d, with the load C_L replaced with a low R (i.e., 50 Ω). (ii) Secondly, HBC receivers are implemented using modern CMOS process technologies having a transistor as an efficient voltage sensor, not an efficient current sensor. Hence, instead of measuring the power gain that requires impedance matching for its maximization and is common in traditional RF-based techniques, the proposed modality uses voltage mode signaling with high-impedance capacitive termination at the receiver end to maximize the efficiency of information exchange between the wearable devices. Besides, the transmitter is designed to have minimum source impedance to maximize the available voltage pickup at the receiver, which otherwise needs to be higher to achieve maximum power gain owing to the high impedance of the human body channel. In addition, the low frequency of operation makes the impedance matching not a necessary step to be followed, as reflections are not of concern in the EQS frequency regime[41]. Based on the above understandings, the input capacitance of the buffer (~2 pF) acts as a load to the receiver.

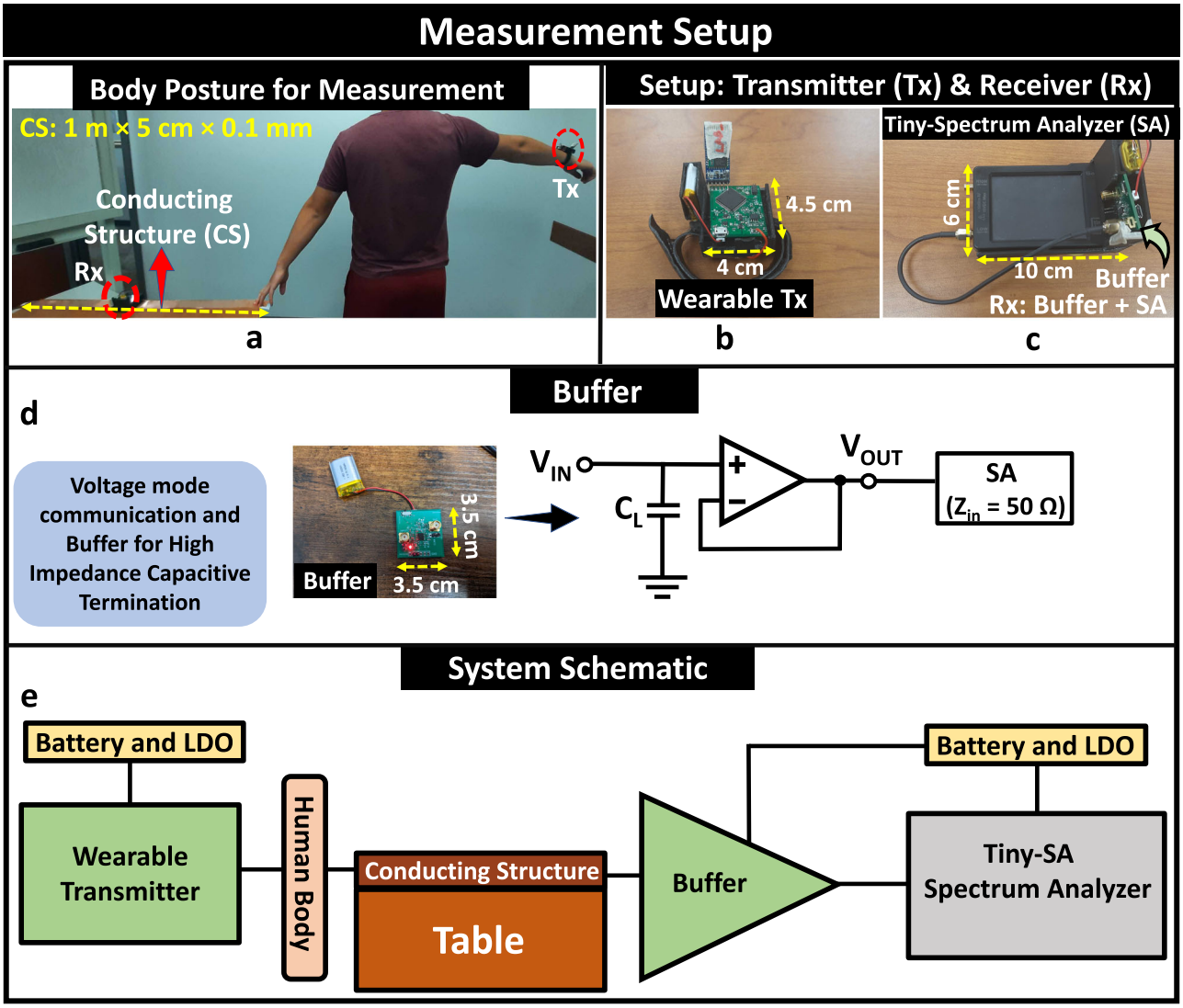

Fig. 13 | Measurement setup. a Subject's body posture during the channel gain measurements: subject with a wrist-worn wearable transmitter (Tx) at one arm is touching the conducting structure (CS: copper tape mounted on a wooden table), with the other arm. The spectrum analyzer (SA) as receiver (Rx) is placed on the CS. **b** Wearable Transmitter. **c** Receiver setup: tiny SA spectrum analyzer together with buffer. **d** Buffer with its schematic for voltage mode communication with high impedance capacitive termination (C_L) **e** Measurement system schematic.

Buffer. A customized buffer with wide operational bandwidth is implemented with an operational amplifier (OPA2836 from Texas Instruments) in unity gain configuration, shown in Fig. 13d. The buffer is housed in a 3D-printed enclosure along with the portable spectrum analyzer and the buffer output is connected to the input of the spectrum analyzer using a SMA cable.

Measurement procedure. Variations in measurements of channel gain with variations in electrode orientation and subject's body posture necessitate consistent electrode configurations with steady body posture, which was confirmed by measuring channel gain with repeatability in measurement readings. The schematic diagram of the measurement system is shown in Fig. 13e. The measurements for HSI is executed with the subject, wearing the Tx setup on the left arm, touched the CS with the right arm, whereas the Rx setup is kept in contact with the CS. Similarly, for the HSHI measurements, another subject holds the Rx while touching the CS. Received voltage measurements were carried out by converting received power levels (P_{Rx}(dBm)), recorded using 50 Ω input impedance TinySA spectrum analyzer with buffer at its input for high-impedance capacitive termination, to peak received voltage V_{Rx} (peak). Eventually, channel gain (G) was evaluated as follows: Channel gain $(G) = 20\log_{10}(\frac{V_{Rx}(\text{peak}-\text{peak})}{V_{Tx}(\text{peak}-\text{peak})})$ for different possible scenarios in HSI and HSHI.

Demonstration setup

A Wi-R Evaluation Board kit by Ixana is used as a transceiver for demonstrating audio streaming over an on-body-to-off-body link. Utilizing capacitive EQS-HBC while being connected to a smartphone to get powered up and programmed, this transceiver module transmits data through the human body. This communication module, configured to transmit at 18.75 MHz with a peak-to-peak voltage level of 2.5 V, sends 64-bit packets of PRBS data while supporting a peak data rate of 1.44 Mbps. While configured as a receiver node, this module is incorporated into a wearable headset. The low BER ($<10^{-3}$) ensures reliable audio transmission. The demonstrated video emphasizes the impact of the proposed link in enabling touch-based non-radiative guided communication over a long channel.

Reporting summary

Further information on research design is available in the Nature Portfolio Reporting Summary linked to this article.

Data availability

The data that support the plots and other findings of this study are provided in this paper and are available from the corresponding author upon reasonable request.

Code availability

Custom codes used to process the data are available from the corresponding author upon reasonable request.

Received: 15 December 2023; Accepted: 12 December 2024;
Published online: 18 February 2025

References

1. Waibel, A. et al. Smart: the smart meeting room task at isl. In: *2003 IEEE International Conference on Acoustics, Speech, and Signal Processing, 2003. Proceedings. (ICASSP'03)*., vol. 4, IV–752 (IEEE, 2003).
2. Sen, S. Socialhbc: social networking and secure authentication using interference-robust human body communication. In: *Proceedings of the 2016 International Symposium on Low Power Electronics and Design*, 34–39 (2016).
3. Pulkkinen, T. et al. Progressive monitoring and treatment planning of diabetes mellitus in smart home environment. In: *2013 IEEE International Conference on Consumer Electronics (ICCE)*, 206–207 (IEEE, 2013).
4. Chatterjee, S. et al. Persuasive and pervasive sensing: a new frontier to monitor, track and assist older adults suffering from type-2 diabetes. In: *2013 46th Hawaii international conference on system sciences*, 2636–2645 (IEEE, 2013).
5. Chiang, S. Y., Kan, Y. C., Tu, Y. C. & Lin, H. C. A preliminary activity recognition of WSN data on ubiquitous health care for physical therapy. In: *Recent Progress in Data Engineering and Internet Technology: Volume 1*, 461–467 (Springer, 2013).
6. Sardini, E. & Serpelloni, M. T-shirt for vital parameter monitoring. In: *Sensors: Proceedings of the First National Conference on Sensors, Rome 15–17 February, 2012*, 201–205 (Springer, 2013).
7. Holz, C. & Baudisch, P. Fiberio: a touchscreen that senses fingerprints. In: *Proceedings of the 26th annual ACM symposium on User interface software and technology*, 41–50 (2013).
8. Holz, C. & Knaust, M. Biometric touch sensing: seamlessly augmenting each touch with continuous authentication. In: *Proceedings of the 28th Annual ACM Symposium on User Interface Software & Technology*, 303–312 (2015).
9. Holz, C. & Bentley, F. R. On-demand biometrics: fast cross-device authentication. In: *Proceedings of the 2016 CHI Conference on Human Factors in Computing Systems*, 3761–3766 (2016).
10. Sato, M., Poupyrev, I. & Harrison, C. Touché: enhancing touch interaction on humans, screens, liquids, and everyday objects. In: *Proceedings of the SIGCHI Conference on Human Factors in Computing Systems*, 483–492 (2012).
11. Harrison, C., Sato, M. & Poupyrev, I. Capacitive fingerprinting: exploring user differentiation by sensing electrical properties of the human body. In: *Proceedings of the 25th annual ACM symposium on User interface software and technology*, 537–544 (2012).
12. Matsushita, N., Tajima, S., Ayatsuka, Y. & Rekimoto, J. Wearable key: device for personalizing nearby environment. In: *Digest of Papers. Fourth International Symposium on Wearable Computers*, 119–126 (IEEE, 2000).
13. Maity, S. et al. Bodywire-hci: enabling new interaction modalities by communicating strictly during touch using electro-quasistatic human body communication. *ACM Trans. Comput. Hum. Interact. (TOCHI)* **27**, 1–25 (2020).
14. Baker, S. B., Xiang, W. & Atkinson, I. Internet of things for smart healthcare: technologies, challenges, and opportunities. *IEEE Access* **5**, 26521–26544 (2017).
15. Kuzlu, M., Pipattanasomporn, M. & Rahman, S. Review of communication technologies for smart homes/building applications. In: *2015 IEEE Innovative Smart Grid Technologies-Asia (ISGT ASIA)*, 1–6 (IEEE, 2015).
16. Mehmood, Y. et al. Internet-of-things-based smart cities: recent advances and challenges. *IEEE Commun. Mag.* **55**, 16–24 (2017).
17. Sen, S., Maity, S. & Das, D. The body is the network: to safeguard sensitive data, turn flesh and tissue into a secure wireless channel. *IEEE Spectr.* **57**, 44–49 (2020).
18. Chatterjee, B., Mohseni, P. & Sen, S. Bioelectronic sensor nodes for the internet of bodies. *Annu. Rev. Biomed. Eng.* **25**, 101–129 (2023).
19. Chatterjee, B., Cao, N., Raychowdhury, A. & Sen, S. Context-aware intelligence in resource-constrained IoT nodes: opportunities and challenges. *IEEE Des. Test.* **36**, 7–40 (2019).
20. Das, D., Maity, S., Chatterjee, B. & Sen, S. Enabling covert body area network using electro-quasistatic human body communication. *Sci. Rep.* **9**, 1–14 (2019).
21. Nath, M., Maity, S., Avlani, S., Weigand, S. & Sen, S. Inter-body coupling in electro-quasistatic human body communication: Theory and analysis of security and interference properties. *Sci. Rep.* **11**, 1–15 (2021).
22. Maity, S., Das, D. & Sen, S. Wearable health monitoring using capacitive voltage-mode human body communication. In: *2017 39th Annual International Conference of the IEEE Engineering in Medicine and Biology Society (EMBC)*, 1–4 (IEEE, 2017).
23. Maity, S., Nath, M., Bhattacharya, G., Chatterjee, B. & Sen, S. On the safety of human body communication. *IEEE Trans. Biomed. Eng.* **67**, 3392–3402 (2020).
24. Bowman, D. A., Kruijff, E., LaViola, J. J. & Poupyrev, I. An introduction to 3-d user interface design. *Presence* **10**, 96–108 (2001).
25. Zhang, Y., Zhou, J., Laput, G. & Harrison, C. Skintrack: using the body as an electrical waveguide for continuous finger tracking on the skin. In: *Proceedings of the 2016 CHI Conference on Human Factors in Computing Systems*, 1491–1503 (2016).
26. Zhou, J., Zhang, Y., Laput, G. & Harrison, C. Aurasense: enabling expressive around-smartwatch interactions with electric field sensing. In: *Proceedings of the 29th Annual Symposium on User Interface Software and Technology*, 81–86 (2016).
27. Fukumoto, M. & Shinagawa, M. Carpetlan: a novel indoor wireless (-like) networking and positioning system. In: *International Conference on Ubiquitous Computing*, 1–18 (Springer, 2005).
28. Park, D. G. et al. Tap: touch-and-play. In: *Proceedings of the SIGCHI conference on Human Factors in computing systems*, 677–680 (2006).
29. Takahashi, M. et al. Earthlings attack! a ball game using human body communication. In: *Proceedings of the 2nd Augmented Human International Conference*, 1–4 (2011).
30. Hessar, M., Iyer, V. & Gollakota, S. Enabling on-body transmissions with commodity devices. In: *Proceedings of the 2016 ACM International Joint Conference on Pervasive and Ubiquitous Computing*, 1100–1111 (2016).
31. Varga, V., Vakulya, G., Sample, A. & Gross, T. R. Enabling interactive infrastructure with body channel communication. *Proc. ACM Interact. Mob. Wearable Ubiquitous Technol.* **1**, 1–29 (2018).
32. Bae, J., Song, K., Lee, H., Cho, H. & Yoo, H.-J. A 0.24-nj/b wireless body-area-network transceiver with scalable double-fsk modulation. *IEEE J. Solid-State Circuits* **47**, 310–322 (2011).
33. Cho, N., Yan, L., Bae, J. & Yoo, H.-J. A 60 kb/s–10 mb/s adaptive frequency hopping transceiver for interference-resilient body channel communication. *IEEE J. Solid-State Circuits* **44**, 708–717 (2009).
34. Maity, S., Das, D., Jiang, X. & Sen, S. Secure human-internet using dynamic human body communication. In: *2017 IEEE/ACM International Symposium on Low Power Electronics and Design (ISLPED)*, 1–6 (IEEE, 2017).
35. Maity, S., Chatterjee, B., Chang, G. & Sen, S. Bodywire: a 6.3-pj/b 30-mb/s- 30-db sir-tolerant broadband interference-robust human body

communication transceiver using time domain interference rejection. *IEEE J. Solid-State Circuits* **54**, 2892–2906 (2019).
36. Maity, S., Mojabe, K. & Sen, S. Characterization of human body forward path loss and variability effects in voltage-mode hbc. *IEEE Microw. Wirel. Compon. Lett.* **28**, 266–268 (2018).
37. Nath, M., Maity, S. & Sen, S. Toward understanding the return path capacitance in capacitive human body communication. *IEEE Trans. Circuits Syst. II: Express Briefs* **67**, 1879–1883 (2019).
38. Datta, A., Nath, M., Yang, D. & Sen, S. Advanced biophysical model to capture channel variability for eqs capacitive hbc. *IEEE Trans. Biomed. Eng*. **68**, 3435–3446 (2021).
39. Maity, S. et al. Bio-physical modeling, characterization, and optimization of electro-quasistatic human body communication. *IEEE Trans. Biomed. Eng.* **66**, 1791–1802 (2018).
40. Avlani, S., Nath, M., Maity, S. & Sen, S. A 100khz-1ghz termination-dependent human body communication channel measurement using miniaturized wearable devices. In: *2020 Design, Automation & Test in Europe Conference & Exhibition (DATE)*, 650–653 (IEEE, 2020).
41. Yang, D., Maity, S. & Sen, S. Physically secure wearable–wearable through-body interhuman body communication. *Front. Electron.* **2**, 807051 (2022).
42. Zimmerman, T. G. Personal area networks: near-field intrabody communication. *IBM Syst. J.* **35**, 609–617 (1996).
43. Park, J. & Mercier, P. P. Magnetic human body communication. In: *2015 37th Annual International Conference of the IEEE Engineering in Medicine and Biology Society (EMBC)*, 1841–1844 (IEEE, 2015).
44. Modak, N., Nath, M., Chatterjee, B., Maity, S. & Sen, S. Bio-physical modeling of galvanic human body communication in electro-quasistatic regime. *IEEE Trans. Biomed. Eng.* **69**, 3717–3727 (2022).
45. Nath, M., Ulvog, A. K., Weigand, S. & Sen, S. Understanding the role of magnetic and magneto-quasistatic fields in human body communication. *IEEE Trans. Biomed. Eng.* **69**, 3635–3644 (2022).
46. Gabriel, S. et al. The dielectric properties of biological tissues: II. measurements in the frequency range 10 hz to 20 GHz. *Phys. Med. Biol.* **41**, 2251–2269 (1996).

Acknowledgements

This work was supported by Quasistatics, Inc. dba Ixana -Grant 40003567.

Author contributions

S.Sen conceived the idea. S.Sarkar, D.Y., and S.Sen conducted the theoretical analysis. D.Y. created the audio demo that inspired the theoretical analysis. S.Sarkar conducted numerical simulations. S.Sarkar and D.Y. performed the experiments. M.N. and A.D. provided suggestions on the theory buildup, numerical simulations, and experiments. S.M. provided guidance during the audio demo preparation. All the authors analyzed the results and reviewed the manuscript.

Competing interests

The authors declare that D.Y., S.M., and S.Sen have a financial interest in Quasistatics, Inc. and the remaining authors declare no competing interests.

Additional information

Supplementary information The online version contains supplementary material available at https://doi.org/10.1038/s44172-024-00333-x.

Correspondence and requests for materials should be addressed to Shreyas Sen.

Peer review information *Communications Engineering* thanks Joonsung Bae and the other, anonymous, reviewer(s) for their contribution to the peer review of this work. Primary Handling Editors: Anastasiia Vasylchenkova and Rosamund Daw.